

Abstract

Effective capturing of solar energy is of immense importance as part of finding a solution for the ever-increasing demand for power coupled with the depletion of resources of fossil fuels. The location of Masdar city in the UAE is associated with relatively high levels of atmospheric dust concentrations. This causes high rates of dust accumulation on solar collectors, which decreases the total energy yields. Therefore, minimizing the amount of dust that accumulates on top of the solar collectors is of great importance for solar energy utilization in general and for the Masdar Initiative and Masdar City in particular.

The objective of this research was to develop a model that describes dust accumulation in order to understand the factors that affect the utilization of PVs in an area with high dust concentrations. We started by developing a simple regression model that describes the maximum power output of a PV, and then using a simple technique we were able to correct for the effect of the incident angle without the need for any experimental setup.

Subsequently, we moved on to tackle the problem of dust accumulation by trying to relate the rate of dust accumulation to different weather conditions. Although our data had a limited time resolution, we managed to describe qualitatively the dust accumulation dependence on several weather parameters. We also proposed a new experimental framework that improves the time resolution of our experimental setup that allows collecting the different parameters that need to be studied in order to be able to develop a quantitative model that describes dust accumulation. A model for dust accumulation combined with a model that describes the PV power output will

enable us to better predict the power output and energy yields on one hand, and to optimize the cleaning of PV modules on the other. Also such a model will help us in developing functionalized coatings that minimize dust accumulation through identifying and understanding the factors that affect dust accumulation.

These functionalized coatings that minimize dust accumulation were investigated as well. An outdoor test for assessing the ability to minimize dust accumulation on PVs of a commercial coating was carried out. Such tests are essential to give us more understanding about the different parameters that need to be taken into account when developing and assessing such coatings.

This research was supported by the Government of Abu Dhabi to help fulfill the vision of the late President Sheikh Zayed Bin Sultan Al Nayhan for sustainable development and empowerment of the UAE and humankind.

Acknowledgments



After two challenging academic years, finally this work has come into realization. The first and the last to thank is Allah, for his blessings and mercy without which I wouldn't have existed and consequently this work wouldn't have existed either.

Thanks and praise to Allah, who blessed me with the most beautiful parents and brother one can ever have, who were there for me; with their love, support and the many prayers they said for me.

I would like to express my appreciation to all who helped in bringing this project into life. Many thanks go to my friends who made my stay in Abu Dhabi enjoyable. Special thanks to Dr. Sameer Abu-Zaid and Mr. Mahran Mohebi from Masdar City for their support and for supplying our group with all the necessary data. I would also like to express my gratitude to Mr. Darryl Myburgh from the Aeronautical Meteorological Department – Abu Dhabi – United Arab Emirates, for supplying us with data that we needed.

Last but not least, I would also like to express my sincere gratitude to my advisors who through the whole journey enlightened me with their knowledge and experience. Thank you Dr. Peter. Thank you Dr. Matteo.

Zaid M. Tahboub

Contents

List of Tables.....	vii
List of Figures	viii
CHAPTER 1	1
1 Introduction	1
1.1 Overview and Motivation.....	1
1.2 Background and Literature Review.....	5
1.2.1 Effect of Dust Accumulation on the Efficiency of Solar Collectors	5
1.2.2 Modeling PV Power Output.....	7
1.2.3 Functional Coating to Provide Self-Cleaning Properties.....	11
1.3 Thesis Organization.....	12
CHAPTER 2	13
2 PV's Maximum Power Output Modeling.....	13
2.1 Introduction and Rationale	13
2.2 Maximum Power Output Model	15
2.3 Assessing The Model's Accuracy: Error Statistics	16
2.4 Data Analysis and Results.....	18
2.4.1 Old Data Analysis	20
2.4.2 New Experimental Setup	22
2.4.3 Development of the Corrected Model.....	25
CHAPTER 3	38
3 Modeling of Dust Accumulation	38
3.1 Theory: Nature of Dust Accumulation.....	39
3.2 Experimental Setup	40
3.3 Analysis.....	42
3.3.1 Performance Criteria.....	42

3.3.2	Deposition and Resuspension of Dust	42
3.3.3	The effect of Wind Speed	45
3.3.4	The Effect of Wind Direction	46
3.4	Preliminary Results	47
3.5	Improving the Current Experiment	48
CHAPTER 4	51
4	Self-Cleaning Surface Testing.....	51
4.1	Methodology	52
4.2	Test Procedures	52
4.2.1	Topography	52
4.2.2	Contact Angle Measurements	54
4.2.3	Optical Properties.....	55
4.2.4	Outdoor Testing	57
4.3	Results and Conclusions.....	59
CHAPTER 5	61
5	Summary and Conclusions	61
5.1	Summary	61
5.2	Conclusions and Recommendations.....	62
5.2.1	Modeling PV Power Output.....	62
5.2.2	Dust Accumulation	63
5.2.3	Functionalized Coatings.....	63
6	Bibliography	65

List of Tables

Table 1 Round noon model statistics	26
Table 2 Statistics of round noon model used to predict power over the whole day	29
Table 3 IAM curves parameters.....	34
Table 4 Summary of the statistics of the models	35

List of Figures

Figure 1 Energy generation share at Masdar City	2
Figure 2 Motives for understanding dust accumulation	3
Figure 3 Incident angle modifier.....	16
Figure 4 September 2008 sample days ($\theta < 50$)	20
Figure 5 Structure in residuals - old data	21
Figure 6 Normalized percentage difference vs. measured power.....	21
Figure 7 Instrumentation – Power Measurement.....	23
Figure 8 Schematic Diagram – Power Measurement	23
Figure 9 Irradiance on the plane of the PV measuring setup.....	24
Figure 10 Back side showing junction boxes	25
Figure 11 Residuals $\theta < 50$	27
Figure 12 Percent normalized difference in power vs. measured power.....	28
Figure 13 Modeled vs. measured power output.....	28
Figure 14 Round noon model over-estimation of power output.....	30
Figure 15 Daily structure in residuals.....	31
Figure 16 Incident angle modifier obtained using the round noon model.....	32
Figure 17 Licor cosine response	33
Figure 18 IAM curve fit.....	34
Figure 19 Modeled vs. measured power for the corrected round noon model	36
Figure 20 Residuals of the corrected round noon model	36

Figure 21 Daily mean dust concentration	41
Figure 22 Time series of the daily change in the normalized energy difference	43
Figure 23 Normalized energy difference	44
Figure 24 Scatter plot of daily change vs. daily average wind speed	45
Figure 25 Scatter plot of daily change vs. daily average wind direction	46
Figure 26 Effect of averaging humidity	49
Figure 27 Wet leaf sensor	50
Figure 28 AFM scan of the uncoated and coated glass cover.....	53
Figure 29 Contact angle of water on glass.....	54
Figure 30 Contact angle of water on the nano-coating	55
Figure 31 Experimental setup for testing for light transmittance	56
Figure 32 Power output of the uncovered and covered Licors	57
Figure 33 Daily Energy output of the coated and uncoated PV	58

CHAPTER 1

Introduction

1.1 OVERVIEW AND MOTIVATION

Effective capturing of solar energy is of immense importance, as part of finding a solution for the ever-increasing demand for power that is coupled with the depletion of resources of fossil fuels.

The plan is to have 100 % of the energy used in Masdar City generated through renewable resources. Figure 1 shows the percentage share of the different planned sources of energy generation at Masdar City. Three out of four of these sources rely on solar energy, namely: evacuated tube collectors, concentrated solar power and photovoltaics, comprising 92 % of the total share.

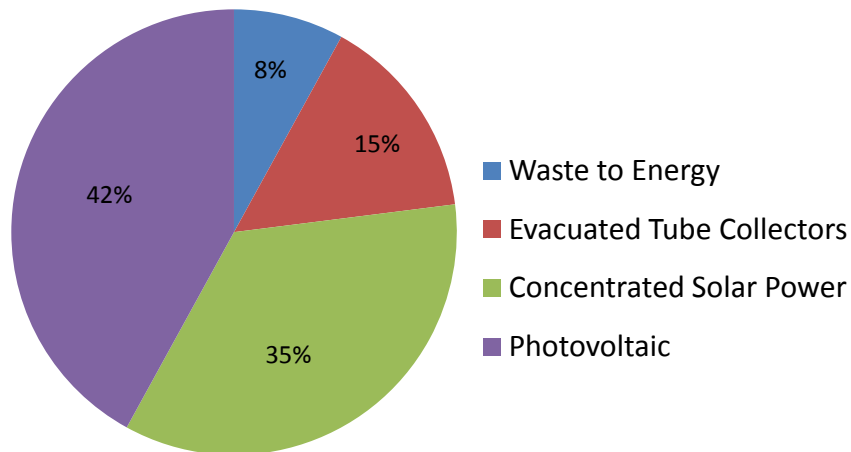


Figure 1 Energy generation share at Masdar City

The location of Masdar City in the UAE is associated with relatively high levels of atmospheric dust concentrations. This causes high rates of dust accumulation on solar collectors. A number of problems are associated with dust accumulation on solar collectors and can be summarized in the following points:

1. A drop in the total energy yield, which reflects on the energy supply of the city.
2. Difficulty in predicting the power output due to dust accumulation losses.
3. Time and cost associated with cleaning solar collectors.

Therefore, minimizing the amount of dust that accumulates on top of the solar collectors is of great importance for the Masdar Initiative and in particular for Masdar City.

In order to be able to resolve the problem of dust accumulation, we first need to understand the dynamics and various factors that affect dust accumulation.

Understanding the factors that affect dust accumulation, namely, weather conditions, is the first step to achieve three important targets: 1- developing accurate power output predictive models by incorporating the drop in power due to dust when modeling the PV's power output, 2- Optimizing the cleaning cost of the solar collectors and 3- Developing coating with self-cleaning properties (summarized in Figure 2).

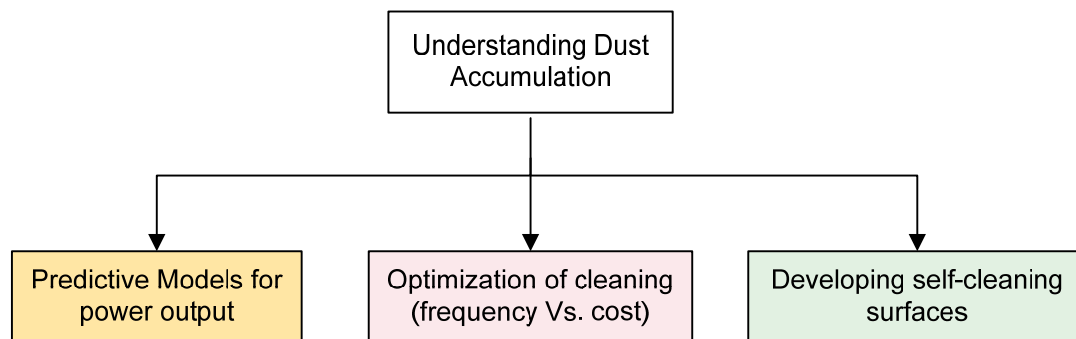


Figure 2 Motives for understanding dust accumulation

In this study, we chose PV modules as our solar collectors since they have a big share of the energy generation at Masdar City.

Relating weather conditions with dust accumulation on PV modules will enable us to come up with better predictive models for the power output of PVs in the sense that these models will include the power losses caused by dust accumulation.

The importance of optimizing the cleaning cost lies in the fact that cleaning is both time consuming and costly. The price of water in a country that depends on desalination as the only source of water is high. Moreover, residue salts in the water used to clean solar collectors may cause some degradation in the collector over time.

Add to that, there is a considerable amount of CO₂ that is related to water production, which for a city that is CO₂ neutral should be taken into account.

The ultimate target is to be able to develop coatings with self-cleaning properties to minimize dust accumulation, thus maximizing the energy yield of PV modules and cutting the cleaning time and cost to a minimum.

The use of such self-cleaning coatings can also be extended to the field of concentrated solar energy. Dust accumulation on concentrating mirrors can decrease their reflectivity and thus the total energy yield.

The current research addresses these three different areas. We try to understand the factors that affect dust accumulation. Developing a model based on weather conditions (such as dust concentration, wind speed and humidity) is our main goal.

Developing and testing a model that describes PV power output comes next. Our model is a regression model that uses simple parameters that can be easily measured (solar irradiation and the modules temperature).

Using easy-to-measure parameters in both models will help in integrating the two models into a powerful PV power output predictive tool.

The understanding that we acquire from the two modeling exercises will help us to identify factors that help us develop coatings that have self-cleaning properties.

1.2 BACKGROUND AND LITERATURE REVIEW

As previously mentioned, the current research addresses three major areas, namely: 1- understanding dust accumulation and correlating dust accumulation with weather conditions, 2- developing a regression model that describes the maximum power output of a PV module as a function of weather conditions, 3- Testing a functionalized coating and its ability to minimize dust accumulation. The following gives a background about the current and previous research in these areas.

1.2.1 EFFECT OF DUST ACCUMULATION ON THE EFFICIENCY OF SOLAR COLLECTORS

Power output from solar collectors are affected by dust accumulation whether solar thermal collectors (e.g. flat plate, evacuated tubes, parabolic trough and Fresnel collectors), or electric solar collectors (e.g. PVs and concentrated PVs). Deposition of dust on the surface of a solar collector can act in two different ways, the first being in reducing the amount of solar radiation by reducing the transmittance of the glass cover in non-concentrating collectors, see [1], [2], [3] and [4], and the second being in reducing the concentrating ability (e.g. reflectivity or convergence) of the concentrating optical system (e.g. mirrors and lenses) in concentrating solar collectors, see [5], and [6].

The drop in power due to dust accumulation varies, and as argued by El-Shobokshy [5], the effect of dust accumulation on the collectors' performance is difficult to generalize because it depends on factors such as: 1- material and size of

dust particles, 2- orientation of the surface with respect to the dominant wind direction, 3- wind speed, 4- humidity, 5- distribution of dust on the surface [g/m^2] and 6- the tilt of the collector from the horizontal. In addition to the previous, other factors can also be argued to contribute to the difficulty in generalizing the effect of dust accumulation such as: 1- the geographical position which affects dust concentration levels 2- seasonal effect, see [7] 3- temperature, 4- collector's surface properties (e.g. material type and surface roughness), 5- amount of sand that is already on the surface (accumulation history) and 6- whether the collector is a stationary or a tracking collector.

In the field of the effect of dust accumulation on PVs, studies have been conducted in controlled environments; few were conducted outdoors and in most of these experiments only deposition of dust is studied. Resuspension of dust is rarely considered in the context of solar energy collection. In health control of ventilation in buildings, Lengweiler [8] proposed a mathematical model that describes the dust deposition velocity and the resuspension rate as a function of the environmental conditions. His investigation was carried under laboratory conditions with the use of a wind tunnel.

In outdoor environments, resuspension has a big effect on the time that is needed for the dust on the PV's surface to reach a certain density; in contrast to indoor experiments that are usually carried out under constant dust flux. As suggested by Goossens [9] a single heavy gust can erode a large percentage of the dust accumulated in the preceding hours, days, or even weeks.

Previous investigations such as the one done by El-Shobokshy [10] showed that, under constant irradiance, the PV's power output (normalized to the maximum power

output) decreases nonlinearly with increasing dust deposition density. Expressing the drop in the PV's normalized power as a function of dust density does not give an indication about the time that will be needed to reach a certain dust density (or power output). Goossens [11] showed similar results and in addition they expressed the drop in power output due to dust accumulation as a function of time. But since the experiment took place under controlled conditions where the PV panels were subjected to an air flow having a constant velocity and a constant dust concentration, the time to reach a certain dust density is not indicative when applied in outdoor conditions, since all conditions were kept constant.

1.2.2 MODELING PV POWER OUTPUT

The ability to predict the power output of PVs is very important for different reasons. Its importance starts from earlier stages of the system design, which helps in predicting annual energy yield in a specific area to know whether PV technology should be invested in or not. It is also important in the operational stage of the PVs. It is a vital tool that enables us to predict power output which is especially important when dealing with utility scale PV fields. It allows us to predict our PV power supply in order to properly allocate the power resources according to the power demand.

There are two types of models in literature that either describe the power output of a PV or the energy output of PVs over a certain period of time. The power output models can be either based on translating the power at a fixed set of reference conditions to another set of conditions or can be based on statistical (regression) analysis [12].

As an example, the PVUSA (Photovoltaics for Utility Scale Applications) project in the 1990's developed a rating methodology for PV performance evaluation which has become popular, and even incorporated into concentrating PV rating standards [13].

The model is as follows:

$$P = G * (A_1 + A_2 * G + A_3 * T_{amb} + A_4 * WS)$$

where:

P = PV array or inverter output [kWdc] or [kWac]

G = Plane-of-array (POA) solar irradiance, broadband measurement [W/m^2]

T_{amb} = Ambient temperature [$^{\circ}C$]

WS = Wind speed [m/s]

A_n = Regression coefficients

The PVUSA method is based on the simplified assumptions that array current is primarily dependent on irradiance and that array voltage is primarily dependent on array temperature, which, in turn is dependent on irradiance, ambient temperature, and wind speed.

One disadvantage of the PVUSA model is that data below a threshold - typically either 500 or 750 W/m^2 - as well as data exhibiting nonstandard behavior are eliminated. A regression is performed on the remaining data to determine the regression coefficients [14]. This means that the accuracy of the model decreases when coefficients generated with high irradiance values are used to predict low

irradiance performance. This reduction is expected since the model does not take into account the effect of the angle of incidence (the angle between the solar beam and the normal to the surface of the PV) [15].

A second model is the ENergy RAting (ENRA) model. This model is also based on regression analysis [12]. The model is as follows:

$$P = A_1 * G + A_2 * G^2 + A_3 * G * \ln(G)$$

where,

P = PV array or inverter output [kWdc] .

G = Irradiance [W/m^2].

A_n = regression coefficients.

The ENRA model also has the disadvantage of using only data above $500 \text{ W}/\text{m}^2$ in computing the regression coefficients. This model does not take into account temperature or spectral changes as well [12], which results in that the model is over predictive [16].

Another model that predicts energy directly rather than power is the Energy Rating at Maximum Ambient Temperature (EMAT) model [16]. EMAT uses only two parameters, namely: plane of array total daily irradiation (H) [$\text{W.h}/\text{m}^2/\text{day}$], and the maximum ambient temperature (T_{max}) [$^{\circ}\text{C}$]. The EMAT model is defined as follows:

$$E = A_1 * H + A_2 * H * T_{\text{max}}^{-2} + A_3 * T_{\text{max}}$$

where,

E = the total daily energy produced by the module in [W.h/day].

H = the total daily irradiation in [W.h/m²/day].

T_{\max} is the maximum ambient temperature [°C].

A_n = regression coefficients.

This model gives a relatively accurate prediction of the energy output of EFG (Edge defined **F**ilm-fed **G**rowth) Si solar cells (on both extreme days, i.e., high and low irradiation, the model predicts exceptionally well and on average days EMAT is accurate to within 10% of the measured energy). ENRA regression model use different values of coefficients for different seasons [16].

In the 90's both NREL and Sandia Labs started to develop more elaborate models that were meant to predict the PV modules and array performance under actual operating conditions [17].

The NREL method is described completely in [18]. It describes how to translate the I-V curve of a PV module using the ratings given by the PV supplier. Suppliers provide I-V curve characteristics under Standard Test Conditions (STC: 1000 W/m², 25°C cell temperature, and AM1.5 Spectrum), which is rarely met in real operating conditions. NREL's method is based on ASTM E 1036-96, with some modifications to increase the accuracy to predict module performance under all conditions.

On the other hand, the method that Sandia Labs developed is completely described in [19]. The Sandia method takes into account the cell temperature, air mass, and angle of incidence in predicting the performance of the PV module. Certain outdoor

testing procedures are used to determine parameters required for modeling the performance of the PV. Sandia's performance model was designed to be applicable to all module technologies, including thin-film and concentrators [17].

There are various other models that describe the power output of a PV module. Skoplaki [20] carried out a comprehensive literature review that discusses and lists a number of the models available. But some of these models do not take into account important parameters such as the cell temperature or the incident angle.

In our work, we try to develop an empirical model that predicts the maximum power output of a PV. Our model lies somewhere in between the comprehensive and elaborate Sandia and NREL models, and between simplified models that don't take into account factors such as the incident angle modifier.

1.2.3 FUNCTIONAL COATING TO PROVIDE SELF-CLEANING PROPERTIES

As mentioned previously, dust plays a significant role in decreasing the PV power output in desert areas. Thus, achieving good energy collection efficiencies requires constant cleaning of the PV modules. Normally water is used in the cleaning process and in arid regions the lack of water calls for alternative cleaning processes that can minimize the amount of water required. Sustainable cleaning methods are particularly important in large scale utilization of PVs.

There is a variety of methods that can be used to clean the PV modules. Manual cleaning is the most obvious, but it comes at the cost of labors and it is the most time consuming method. Automatic cleaning, using special robots, is also an option that is studied.

An alternative that is being extensively investigated relies on the use of self-cleaning coatings that minimize dust accumulation. Studies show that super-hydrophobic surfaces exhibit self-cleaning properties [21-23]. This is achieved by utilizing the high water contact angles that cause water on the surface to form almost spherical droplets that readily roll away carrying dust and dirt with them [24].

1.3 THESIS ORGANIZATION

In chapter 2, we will suggest a model that can be used to predict PV's maximum power output based on regression analysis. Then we will explain the methodology that we used to correct for the effects of the incident angle and spectrum mismatch.

In chapter 3, we will show the methodology that we developed in order to model the dust accumulation as a function of weather conditions. We will discuss why we were not able to statistically validate our model and ways to improve the experimental setup in order to be able to develop a dust accumulation model that can be statistically verified.

In chapter 4, we present the results of testing a commercial self-cleaning surface. We highlight the methodology that we used in our experiment and the rationale behind our approach.

Conclusions of this thesis and recommendations for future work will be presented in chapter 6.

CHAPTER 2

PV's Maximum Power Output Modeling

The ability to predict the power output of PVs is very important for different reasons. Its importance starts from early stages of the system design. Prediction of the energy yields in a specific area will help decision makers to assess the option of investing in PV technology. Its importance carries on to predicting the power output at any given time which is important for any grid connected PV farm.

2.1 INTRODUCTION AND RATIONALE

As we mentioned in chapter 1, there are different models that describe the performance of PVs under variable working conditions. One of the most elaborate models is the model developed by Sandia [19], which describes the I-V curve at any

operating condition, and is applicable to all PV technologies. On the other hand, a lot of models (see [20]) describe to a high accuracy the power output of a PV, but do not take into account the effect of angle of incident and the solar spectrum, which causes the presence of structure in the residuals of the model which should be absent in any regression model.

We developed a simple model that describes the maximum power output of a PV based on the physics of a PV. Using a simple approach we can correct for the incident angle modifier without the use of outdoor experiments. Moreover, by utilizing a PV based irradiation measuring device we were able to correct for the spectrum mismatch [25], [26].

The idea used to correct for the effect of angle of incidence is to use data around solar noon to estimate the coefficients of the regression model. The time around noon is selected since the effect of incident angle is minimal. Then we use this model to estimate the power output of the entire data. Since this model (round noon) does not take into account the incident angle effect, we would expect that the predicted power values using this method to be higher than the actual values at high incident angles (i.e. mornings and evenings). A correction curve then can be obtained by dividing the actual measured output by the modeled output. This correction curve represents the incident angle modifier curve (IAM) which in our case is defined as:

$$IAM = \frac{\text{Measured output}}{\text{Modeled output (using data around noon)}}$$

2.2 MAXIMUM POWER OUTPUT MODEL

We propose a regression model that describes the maximum power output of PVs.

Our model is:

$$P = \begin{cases} A_1 * G * \ln(G) + A_2 * G^2 + A_3 * G * (T + A_4) & , \quad \theta < 60 \\ (A_1 * G * \ln(G) + A_2 * G^2 + A_3 * G * (T + A_4)) * IAM, & \theta \geq 60 \end{cases}$$

where,

P: Maximum power output of a PV [W/m²]

G: Plane of array irradiance [W/m²]

T_c: Cell temperature [°C]

A_n: Regression coefficients

IAM: Incident angle modifier

θ: Incident angle [degrees]

The term [$A_1 * G * \ln(G)$] can be understood when we know that under a constant temperature the PV's open circuit voltage is logarithmically proportional to the short circuit current which in turn is linearly proportional to the irradiance [27]. The [$A_2 * G^2$] term represents the resistive electrical loss (I^2R loss). The third term [$A_3 * G * (T + A_4)$] takes into account the effect of temperature on the PV.

Note that the model was corrected for the incident angle effect only for incident angles larger than 60 degrees where the optical losses are significant. Figure 3 represents a typical incident angle modifier curve.

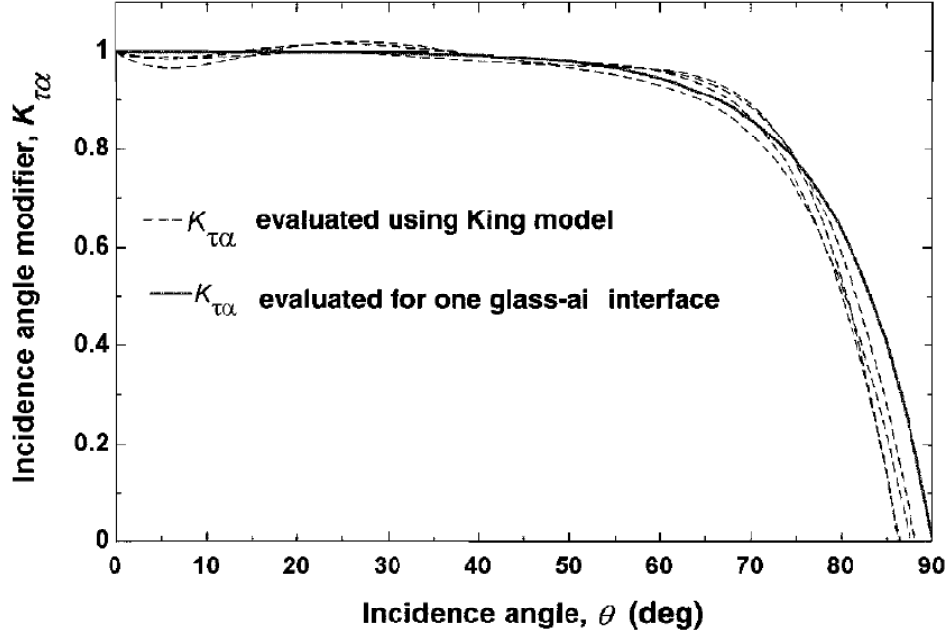


Figure 3 Incident angle modifier [28]

2.3 ASSESSING THE MODEL'S ACCURACY: ERROR STATISTICS

To assess the accuracy of the predictive model, we used the following criteria (based on [29]):

- 1- Root Mean Square Error (RMSE).
- 2- Mean Bias Error (MBE).
- 3- Mean Absolute Error (MAE).
- 4- The coefficient of determination (R^2).

And they are defined as follows:

$$RMSE = 100\% \times \left(\frac{1}{n} \sum_{i=1}^n (y_i - x_i)^2 \right)^{1/2} \div \left(\frac{1}{n} \sum_{i=1}^n x_i \right)$$

$$MBE = 100\% \times \left(\frac{1}{n} \sum_{i=1}^n (y_i - x_i) \right) \div \left(\frac{1}{n} \sum_{i=1}^n x_i \right)$$

$$MAE = 100\% \times \left(\frac{1}{n} \sum_{i=1}^n |y_i - x_i| \right) \div \left(\frac{1}{n} \sum_{i=1}^n x_i \right)$$

$$R^2 = 1 - \left[\left(\sum_{i=1}^n (y_i - x_i)^2 \right) \div \left(\sum_{i=1}^n y_i - \bar{y}_i \right) \right]$$

where,

y_i : measured value.

\bar{y}_i : mean of all measured values.

x_i : modeled value.

n : number of data point.

RMSE is a measure of the variation of the modeled values from the measured values.

MBE represents the average deviation of the modeled values from the measured

values. MAE provides the average absolute deviation of the modeled values from the

measured values. RMSE and MAE are always positive, whereas MBE can be either

positive or negative. R^2 is a measure that indicates how well a model predicts [30].

Although the R^2 value provides a useful indication of the accuracy of the model, it is

also important to look closely at the residual values.

It is important to analyze residuals based on a number of factors, including the following [30]:

- 1- Response variable: There should be no trends in residual values over the range of the response variable, that is, the distribution should be random.
- 2- Frequency distribution: The frequency distribution of the residual values should follow a normal distribution.
- 3- Observation order: There should be no discernable trends based on when the observations were measured.

2.4 DATA ANALYSIS AND RESULTS

In this section we will show how we used real power data in finding the coefficients of our regression model. We will then explain the methodology that we used to obtain the incident angle modifier (IAM) curve. We will also show how the incident angle modifier corrected model compares to the original model and how it performs by showing the different statistical measures that we used to assess the model.

It should be noted that we did the analysis on two sets of data. The first set of data was already available and was given to us by Masdar City. It consisted of:

- 1- Power output measurements.
- 2- Plane of array irradiation.
- 3- PV's back temperature.

Note that the back temperature was converted into the cell temperature using the following empirical formula [19]:

$$T_c = T_b + (G/G_o) \Delta T$$

where,

T_c : PV's cell temp. [$^{\circ}\text{C}$]

T_b : Measured PV's back-surface temp. [$^{\circ}\text{C}$]

G : Solar irradiation [W/m^2]

G_o : Reference solar irradiation [$1000 \text{ W}/\text{m}^2$]

ΔT : Temperature difference between the cell and the module back surface at an irradiance level of $1000 \text{ W}/\text{m}^2$ (This temperature difference is typically 2 to 3 $^{\circ}\text{C}$ for flat-plate modules in an open-rack mount).

As will be shown in the analysis, the regression model that we developed using Masdar City's set of data had a statistical problem in its residuals. When we looked at the residuals (measured power – modeled power), there was a clear structure, and as explained in the previous section, residuals from regression models should be randomly distributed when plotted as a time series. Therefore this led us to take the decision of repeating the experiment where we carried out our own instrumentation and measurements. The parameters measured in the new experiment were the same as those measured in the old experiment. The equipment used in the new experiment was setup carefully and with rigor.

2.4.1 OLD DATA ANALYSIS

As we mentioned previously, we started developing the model using data that was given to us by Masdar City. The problem was the presence of a structure in the residuals.

Figure 4 shows the measured and modeled power output of two sample days from September 2008. It can be seen that the modeled power output lags the measured power (indicated by the red arrows).

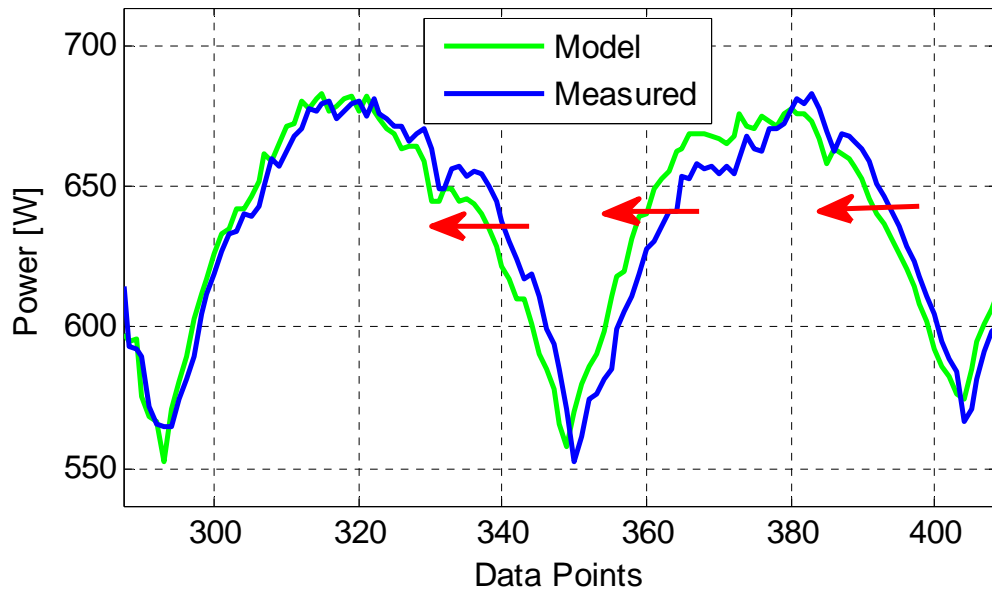


Figure 4 September 2008 sample days ($\theta < 50$)

This lag in the model resulted in a clear trend in the residuals as can be seen in Figure 5. The red lines emphasize the structure trend in the residuals.

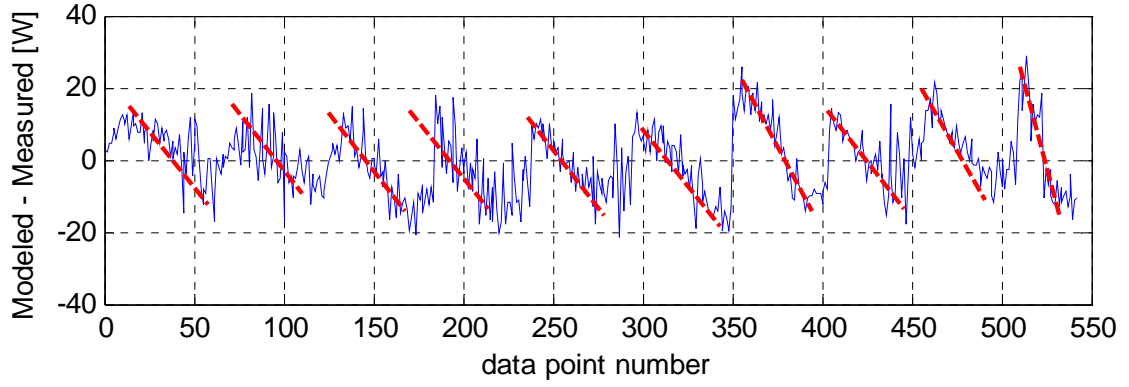


Figure 5 Structure in residuals - old data

Figure 6 shows the normalized percentage difference between the measured and modeled power output having values of $\pm 4\%$.

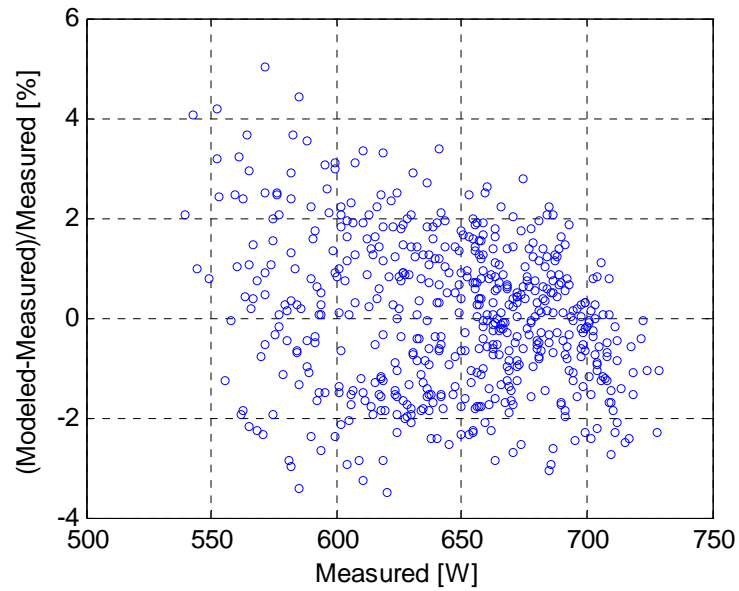


Figure 6 Normalized percentage difference vs. measured power

We believe that this structure might have been caused by several reasons such as:

- 1- Misalignment of the pyranometer relative to the plane of array (POA) that was used to measure the plane of array (POA) irradiation.
- 2- Errors in measuring the PV's back temperature.

Therefore, this led us to taking the decision of repeating the experiment in order to try to eliminate these potential sources of errors.

2.4.2 NEW EXPERIMENTAL SETUP

The new experiment was conducted using the same PV modules as the old experiment. The difference was in the instrumentation used. Both experiments were conducted in the international PV test field located at Masdar city, Abu Dhabi (latitude: 24.4, longitude: 54.6). A Mono-crystalline PV module connected to the grid through a maximum power point tracker (MPPT) was tested. The module consisted of six 1.60 [m] X 0.8 [m] identical panels, making the total area of the module equal to 7.68 [m²]. The module was fixed at a slope of 20 degrees, and were facing true south (surface azimuth of 0 degrees).

In the new experiment, the module's voltage and current output were recorded every 6 seconds for the entire period of the test. The current was measured using a Hall Effect transducer (LEM), and the voltage was measured using a simple voltage divider. Figure 7 shows the current and voltage sensing elements. Figure 8 shows the schematic diagram of the measuring circuit.

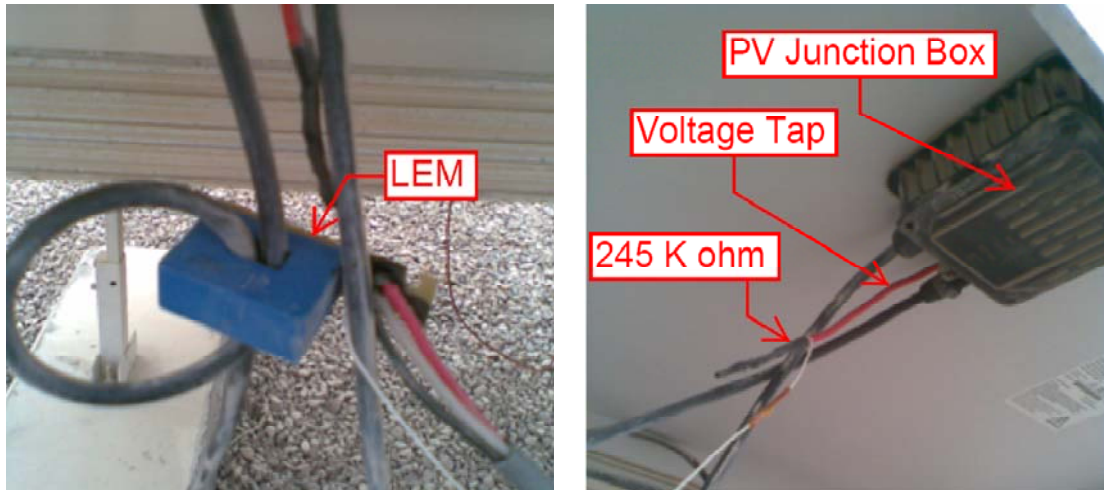


Figure 7 Left - LEM current transducer. Right - Voltage tap in the PV junction box.

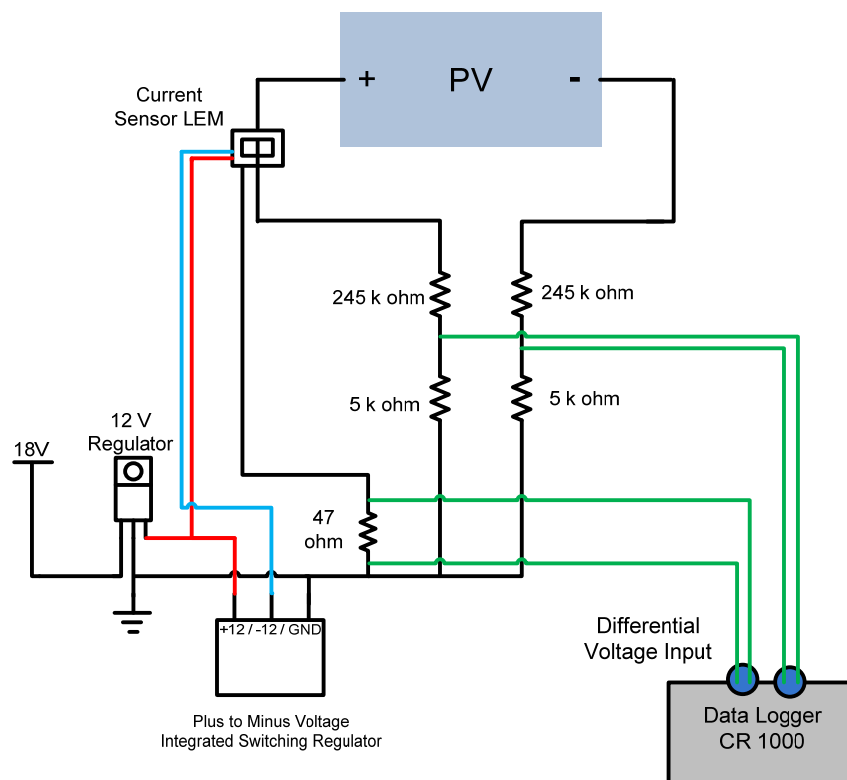


Figure 8 Power measuring circuit

The modules' back temperature was measured by means of ten temperature sensors (k-type thermocouples) fixed at the back side of the module at random positions. An average of the ten readings was used for modeling.

To measure the plane-of-array solar irradiation (POA), two types of sensors were used: 1- a thermopile type pyranometer (CMP22), and 2- four Silicon photovoltaic based pyranometers (Licor).

As we mentioned previously, Licors were used to correct for the spectral mismatch. The CMP22 was used as a reference pyranometer.

Figure 9 and Figure 10 show the front side and the back side of the experimental setup.



Figure 9 Irradiance on the plane of the PV measuring setup

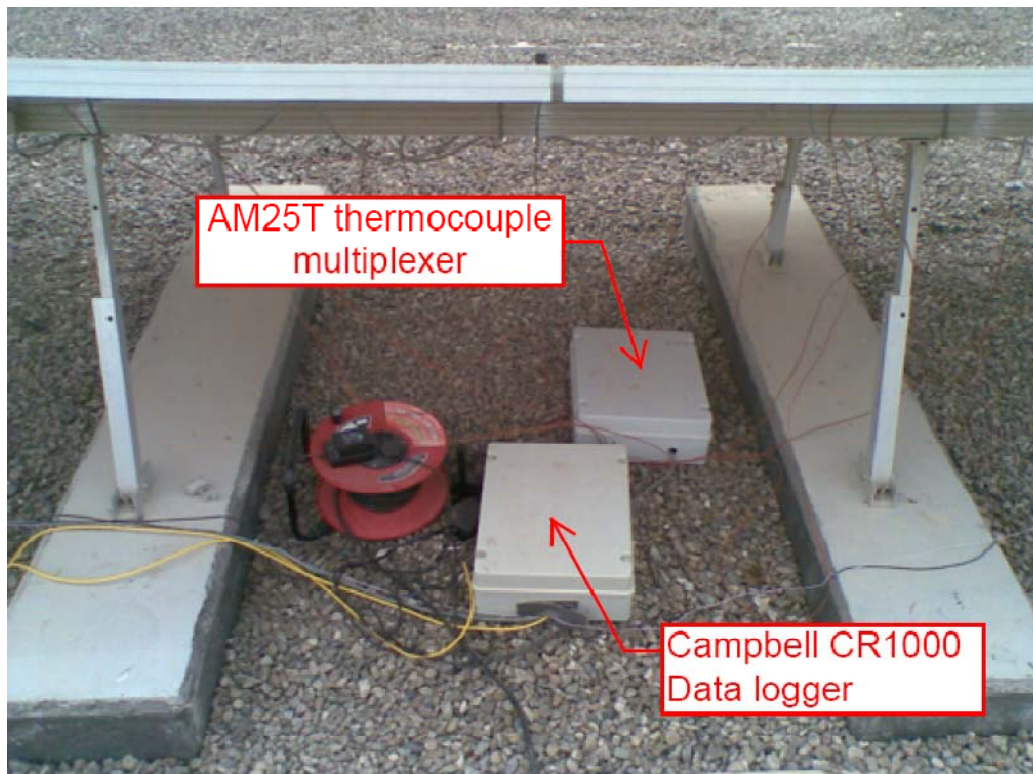


Figure 10 Back side showing junction boxes

2.4.3 DEVELOPMENT OF THE CORRECTED MODEL

As mentioned previously, the idea is to develop a model that uses data measured around the solar noon in order to eliminate the effect of the incident angle. Afterwards, this model is used to predict the power over the whole day and an incident angle modifier curve can then be obtained and the model can be corrected accordingly.

It should be noted that data in which the incident angle θ was larger than 50° in the afternoon was not used in the analysis to avoid the problem of shading caused by nearby buildings.

Following, we will explain the methodology that was used to develop our model.

We start by using data points around the noon (i.e. $\theta < 50$) where the effect of the angle of incidence is negligible. We found our regression coefficients. Table 1 summarized the regression model coefficients and the statistical measure values:

Table 1 Round noon model statistics

Parameter	Round noon model
A1	0.020
A2	-2.360e-5
A3	3.682e-4
A4	35.31
RMSE	1.0714
MBE	-3.55e-5
MAE	0.8605
R^2	0.9803

Figure 11 shows the residuals of the model. Note that the residuals are randomly distributed and that there is no structure observed.

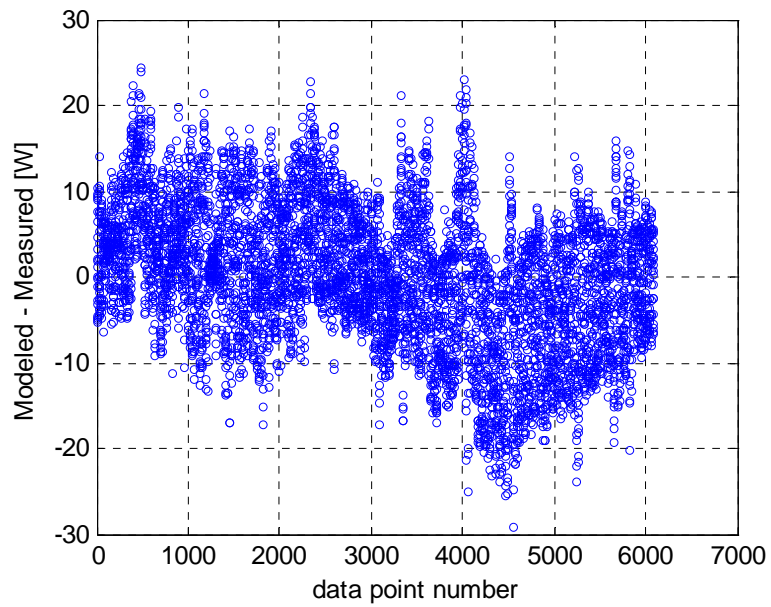


Figure 11 Residuals $0 < 50$

When plotting the normalized power difference against the measured power, it can be noted that the model predicts within $\pm 3\%$ of the measured power output. This is depicted in Figure 12.

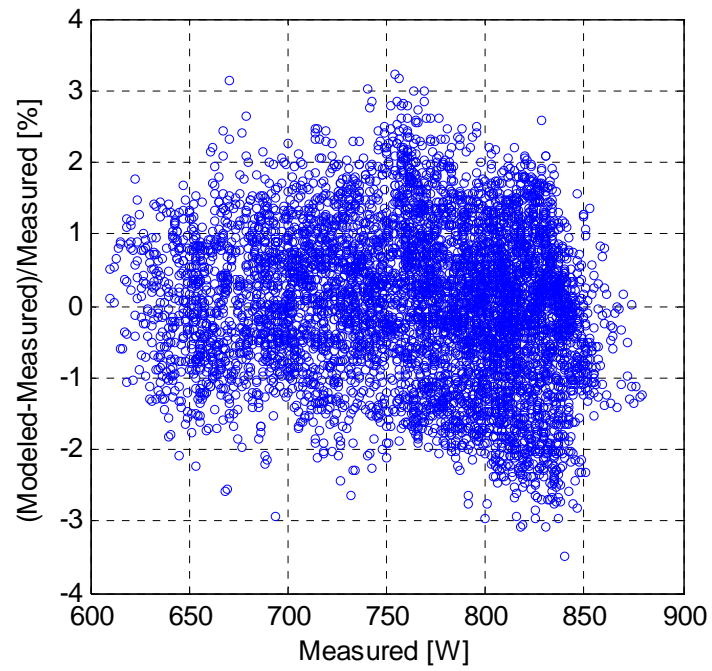


Figure 12 Percent normalized difference in power vs. measured power

Figure 13 shows the well agreement between the modeled and the measured power output. The red line represents the $y = x$ line.

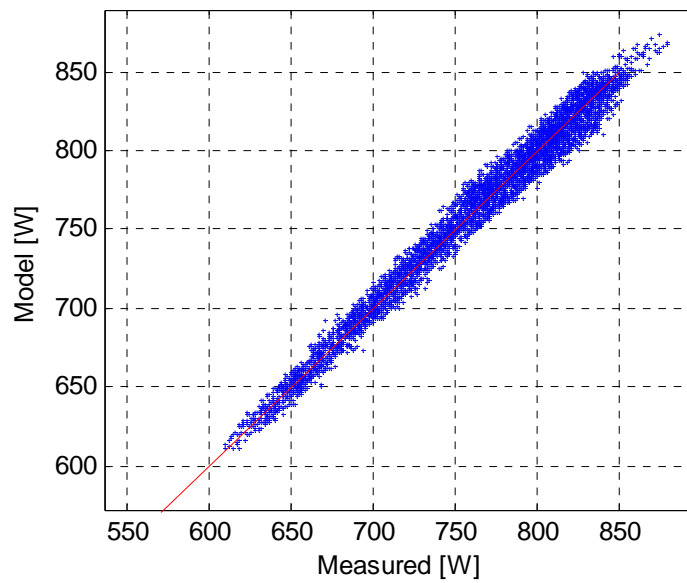


Figure 13 Modeled vs. measured power output

The next step in developing our regression model was using the model that we developed using data around noon (with the same values of coefficients) to predict the power output over the whole day (using all data points). Since we only used data around the noon in the first step, our model does not take into account the effect of the incident angle and thus we expect that the model will over-estimate the power output when used to predict the power output over the entire day. The power output over-estimation will take place where the effect of the incident angle is significant (i.e. in the mornings and afternoons or in another words at large values of incident angle).

Table 2 summarizes the statistics of using the round noon model to estimate the power during the entire day. Notice the significant increase in the RMSE, MBE and MAE. This is expected since the round noon model does not take into account the effect of incident angle.

Table 2 Statistics of round noon model used to predict power over the whole day

Parameter	Round Noon Model	All data using round noon model
A1	0.020	Same
A2	-2.360e-5	Same
A3	3.682e-4	Same
A4	35.31	Same
RMSE	1.0714	3.1674
MBE	-3.55e-5	1.3727
MAE	0.8605	2.0905
R ²	0.9803	0.9956

Figure 14 is a plot of the modeled power versus the measured power. The red line represents the $y = x$ line. It is clear that at low power values (which represents mornings and evenings) the model over estimates the power output. The reason is that the round noon model does not model the effect of the incident angle.

Figure 15 clearly depicts the structure in the residuals of the round noon model when used over the entire day.

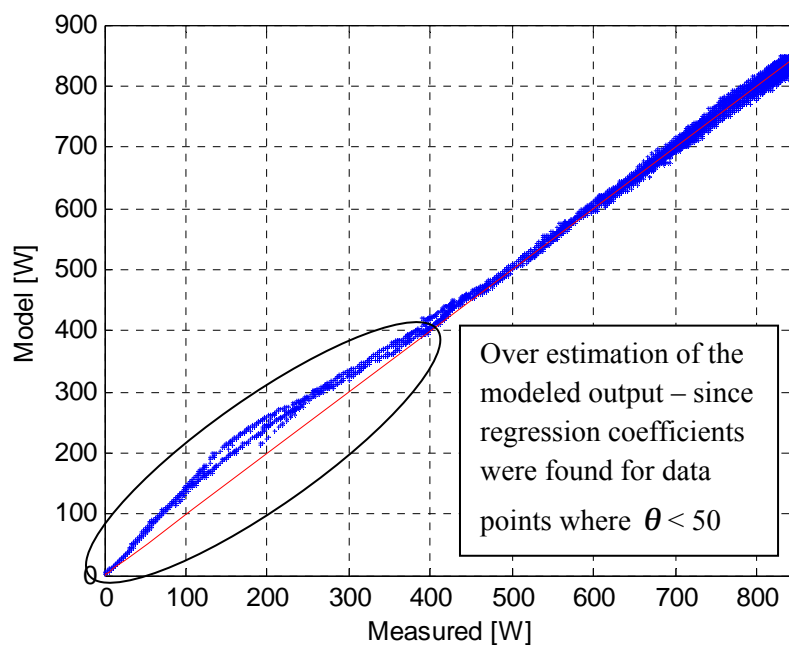


Figure 14 Round noon model over-estimates power output during morning and afternoon

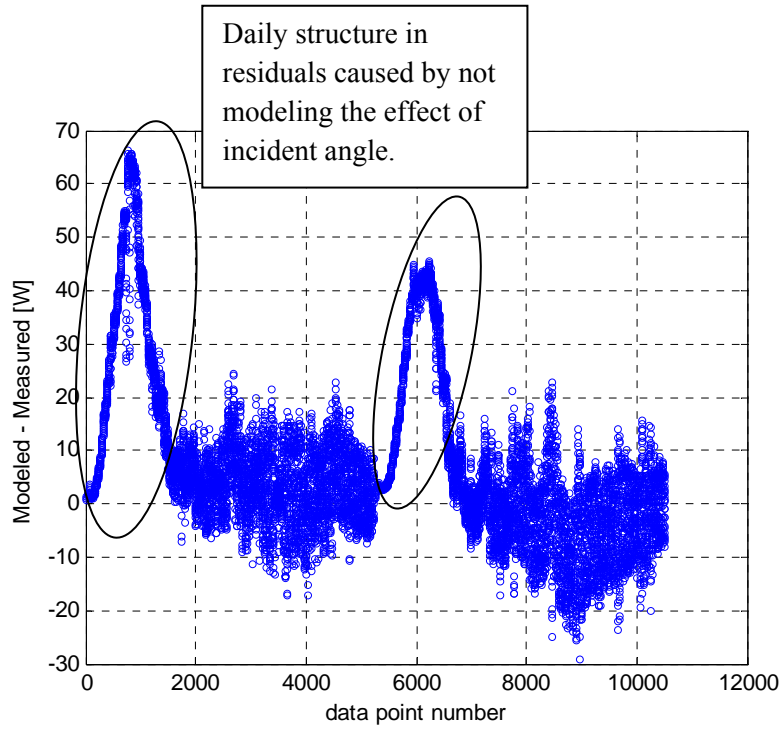


Figure 15 Daily structure in residuals when estimating the daily power output using the round noon model

The next step now is to correct the round noon model for the effect of incident angle by introducing the incident angle modifier curve (IAM) as it was previously defined:

$$IAM = \frac{\text{Measured output}}{\text{Modeled output (using data around noon)}}$$

This resembles the use of a two axis tracker to find the relative difference in performance between a PV mounted on the tracker and another fixed PV due to the effect of the incident angle. Using a tracker will eliminate the effect of the incident angle since the incident angle would be equal to zero all the time.

Our incident angle modifier curve can now be plotted by plotting the ratio of the measured power output to the modeled power output using the round noon model against the incident angle θ . Figure 16 shows the incident angle modifier curve obtained by this method. Note that the effect of the incident angle becomes significant for $\theta \geq 60^\circ$.

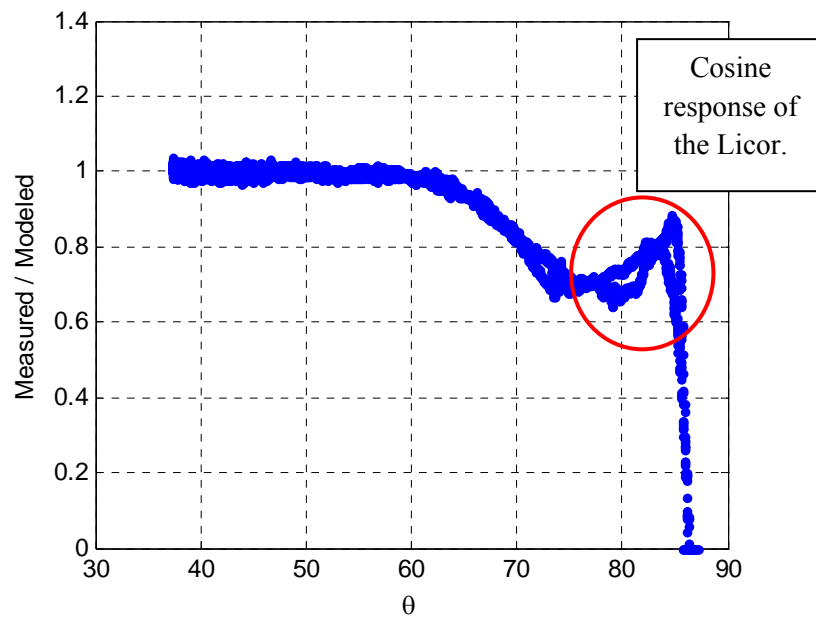


Figure 16 Incident angle modifier obtained using the round noon model

When we compare this curve with the typical IAM curve depicted in Figure 3, we can see a difference indicated by the red circle in Figure 16. This difference accounts for the cosine response of the Licor [31]. A typical cosine response of a Licor is shown in Figure 17.

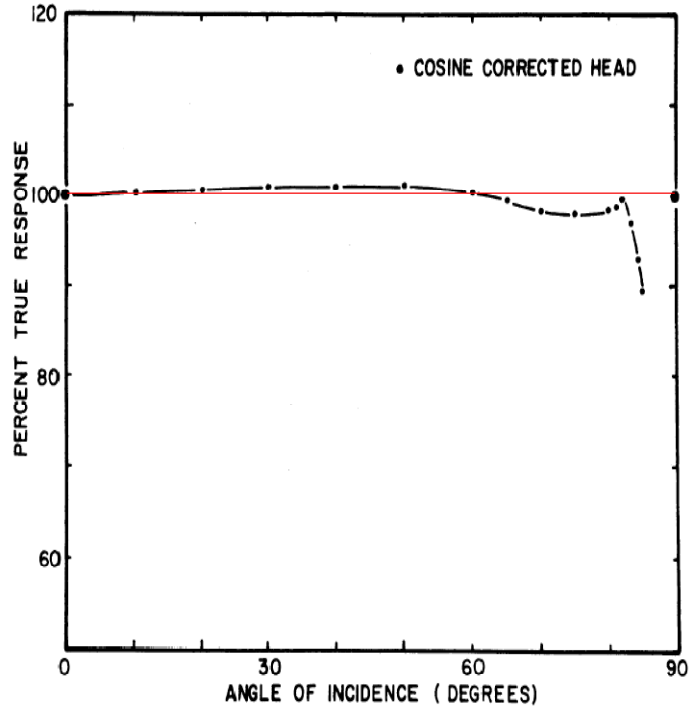


Figure 17 Licor cosine response [31]

Curve fitting was used to find a function that describes the IAM curve. We used two IAM curves to get better fits: one for $60 < \theta < 75$ called IAM 1 and another for $75 < \theta < 85$ called IAM 2.

Following is a summery about the two incident angle curves, and they are visualized in Figure 18.

$$IAM\ 1 = P_1 * \theta^3 + P_2 * \theta^2 + P_3 * \theta + P_4 \quad ,\ 60 < \theta < 75$$

$$IAM\ 2 = P_1 * \theta^2 + P_2 * \theta + P_3 \quad ,\ 75 < \theta < 85$$

Table 3 IAM curves parameters

Parameter	IAM 1	IAM 2
Range	60 – 75	75 - 85
P_1	0.0001009	0.001398
P_2	-0.02134	-0.2125
P_3	1.477	8.773
P_4	-32.63	-
SSE	0.4562	1.564
R-square	0.971	0.4608
Adjusted R-square	0.971	0.4598
RMSE	0.01624	0.03711

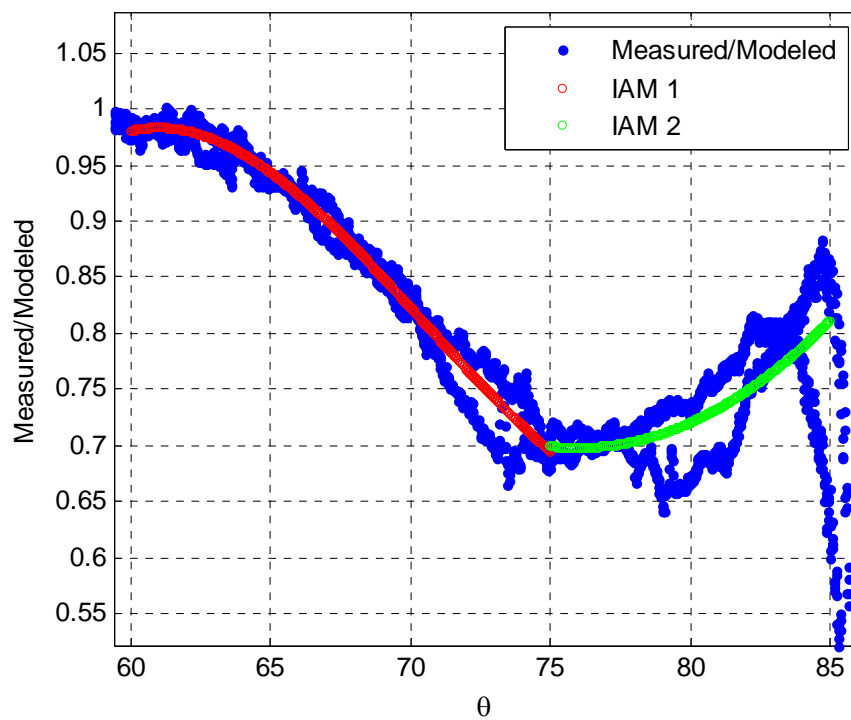


Figure 18 IAM curve fit

The next step in our modeling is to apply the two IAM curves to the round noon model over their specified ranges.

There is a significant improvement in the accuracy of using the corrected round noon model to predict the power output of the entire day especially at large values of θ .

Table 4 compares the statistics of the round noon model, the predicted values of the entire day using the round noon model and the corrected round noon model.

Figure 19 shows the modeled versus measured power output in the case of using the corrected round noon model. Notice the close agreement of the modeled and measured power values at high values of θ (i.e. in the mornings and afternoons; low power output).

Table 4 Summary of the statistics of the models

Parameter	Round noon model	All data using round noon model	Corrected round noon model
A1	0.020	Same	Same
A2	-2.360e-5	Same	Same
A3	3.682e-4	Same	Same
A4	0.013	Same	Same
RMSE	1.0714	3.1674	1.2091
MBE	-3.55e-5	1.3727	0.0938
MAE	0.8605	2.0905	0.9138
R ²	0.9803	0.9956	0.9994

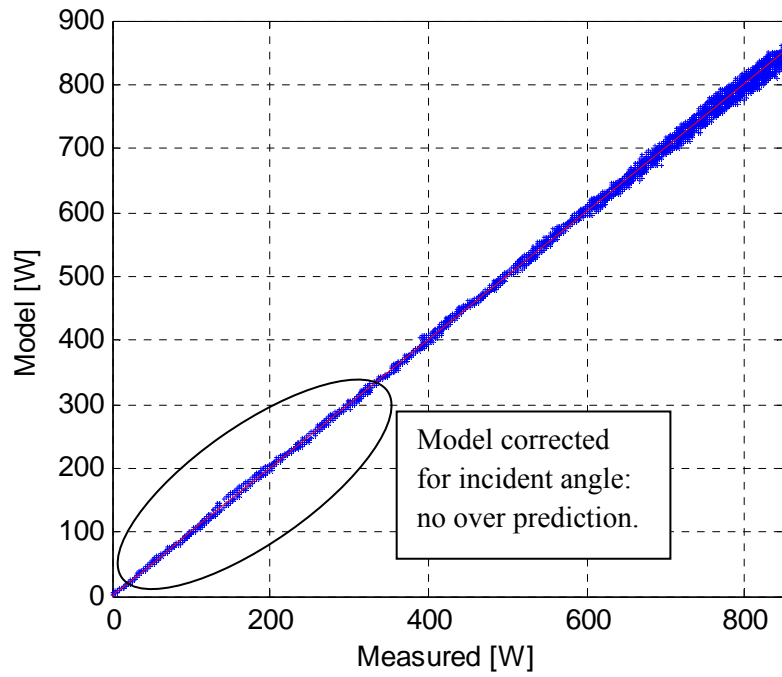


Figure 19 Modeled vs. measured power for the corrected round noon model

When looking at the residuals, we can see that the structure that was present previously disappeared since the model now describes the effect on the incident angle.

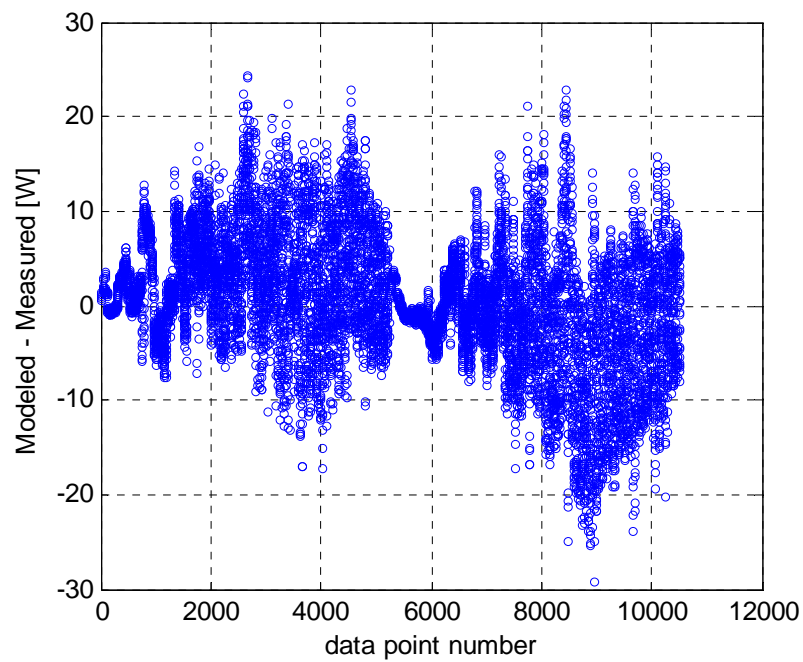


Figure 20 Residuals of the corrected round noon model

Data collection is still taking place. The model should be further verified by using a year's data of power output. Also the model can be generalized to be used with different PV technologies. This needs data collection of the power output of different PV technologies and testing and verifying them again modeled power output.

CHAPTER 3

Modeling of Dust Accumulation

Predictive modeling of PV power output is of immense importance. In some parts of the world, dust accumulation must be taken into account; otherwise the models tend to be over predictive. In this chapter we highlight the importance of considering the resuspension of dust in modeling dust accumulation. We will describe the methodology that we followed and the shortcomings of our experiment. We will highlight ways of improving the experiment in order to be able to statistically validate our model.

3.1 THEORY: NATURE OF DUST ACCUMULATION

Dust deposition is the third phase of wind erosion. Dust emission generated by wind erosion is the main source which affects the atmospheric radiation balance in direct methods (through scattering and absorbing various radiation components) as well as indirect methods (through modifying the optical properties and lifetime of clouds). Wind erosion is a complex process governed by numerous factors that can be classified as: atmospheric conditions (e.g. wind, precipitation and temperature), soil properties (soil texture and composition), land-surface characteristics (e.g. topography, moisture and aerodynamic length) and land-use practices (e.g. farming, grazing and mining). The physics of wind erosion is complex and is so far not fully understood. Wind erosion has three distinct phases namely: 1- particle entrainment (by aerodynamic lift, saltation bombardment and disaggregation), 2- transport and 3- deposition (dry and wet deposition) [32].

There are two fluxes that result in a net dust accumulation, namely: dust deposition and dust resuspension. Dust deposition is the settling of particles in air on a certain surface and is characterized by an overall deposition velocity. There are five different mechanisms in which deposition can take place: 1- gravitational settling, 2- Brownian motion, 3- eddy turbulent diffusion, 4- electrostatic forces and 5- thermophoresis (or thermodiffusion) [8].

Resuspension is the removal of the accumulated dust from the surface back to the air. To remove a dust particle from the surface, a force is needed to counteract the adhesion force between the dust and the surface.

The main adhesion forces are: Van Der Waals force, electrostatic force and surface tension of the adsorbed liquid film. These forces are affected by the material, shape, and the size of particles: the material, the roughness and the contamination of the surface: the relative humidity; the temperature; the duration of contact; and the initial velocity ([33] as cited in [8]). Counteracting forces can be of mechanical, centrifugal, vibrating or hydrodynamic nature [8].

3.2 EXPERIMENTAL SETUP

Our experiment is conducted in the international PV test field located at Masdar City, Abu Dhabi (latitude: 24.4, longitude: 54.6). We compare the performance of a *test* PV module against a *control* PV module. The two modules are identical¹ and are connected to the grid through separate maximum power point trackers. Their maximum power output together with weather data was recorded every 10 minutes².

Data collection was made over a period of 10 months (beginning of September, 2008 until the end of June, 2009).

Dust concentration in the atmosphere was estimated based on hourly visibility data (courtesy of Abu Dhabi's Airport) using the empirical formula presented by Shao ([34] as cited in [35]):

¹ On a clear day where both modules are clean, $b = P_{\text{Control PV}} / P_{\text{Test PV}} = 1.003$, and the coefficient of variation of the RMSE for $(P_{\text{Control PV}} - b * P_{\text{Test PV}}) / P_{\text{Control PV}} = 0.41\%$. (figures for a sample day: 12th, Dec 2008).

² Experimental setup and data acquisition was done by Masdar City under the MASDAR PV Competition Test Field. With their permission, we used the data set in efforts to develop a dust accumulation model.

$$C = \begin{cases} 3802.29 V^{-0.84}, & V < 3.5 \text{ km} \\ \exp(-0.11 V + 7.62), & V \geq 3.5 \text{ km} \end{cases}$$

where C is dust concentration in $[\mu\text{g.m}^{-3}]$, and V is visibility in $[\text{km}]$. Figure 21 shows the daily mean atmospheric dust concentration during the test period based on the visibility data and the foregoing model.

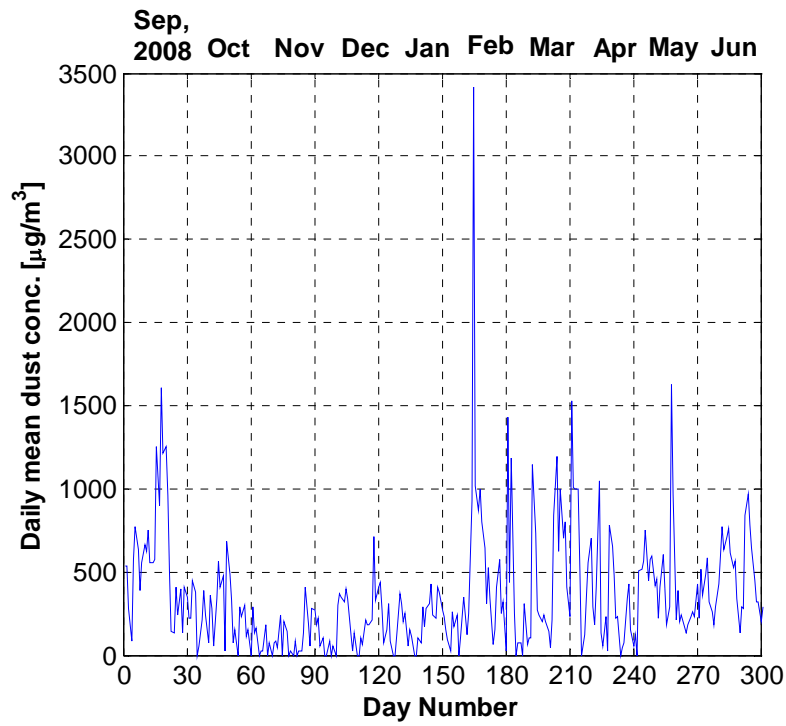


Figure 21 Daily mean dust concentration

3.3 ANALYSIS

3.3.1 PERFORMANCE CRITERIA

When the control PV is clean, any difference in energy produced by the two PVs is due to dust accumulation only since the test and control PVs are identical and operate under the same conditions. We used the normalized energy difference as an indication of the dust accumulation.

$$\text{Normalized Energy Difference (NED)} = \frac{\text{Energy}_{\text{Control PV}} - \text{Energy}_{\text{Test PV}}}{\text{Energy}_{\text{Control PV}}} [\%]$$

Where, $\text{Energy}_{\text{Control PV}}$ is the daily energy generated by the control PV, and $\text{Energy}_{\text{Test PV}}$ is the daily energy generated by the test PV.

3.3.2 DEPOSITION AND RESUSPENSION OF DUST

The deposition and resuspension processes occur in parallel which makes measuring of each process individually impossible [8]. Nevertheless a net flux over a certain period of time can be defined. Thus, for example, if the normalized energy difference between the control and test PV on day (n) was lower than that on day (n+1) we can say that we had a *net deposition* flux on day (n), and if it was higher, then we can say that we had a *net resuspension* flux on day (n).

To summarize:

$$\text{Daily Net Flux} = \begin{cases} \text{Deposition,} & \text{daily change} > 0 \\ \text{Resuspension,} & \text{daily change} < 0 \end{cases}$$

Where, the *daily change* is the change in the normalized energy difference (NED) between two consecutive days (i.e. $NED(n+1) - NED(n)$, where n is the day number).

Figure 22 depicts the time series history of the daily net flux. The net deposition and resuspension fluxes have approximately equally spaced distribution with time, which indicates that resuspension has a considerable effect on the accumulated dust density as a function of time.

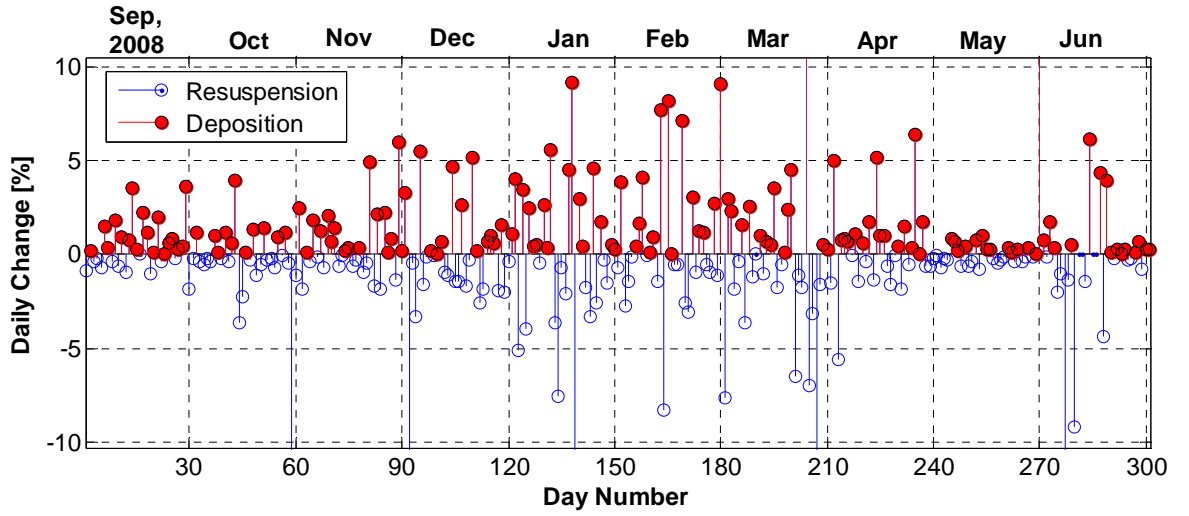


Figure 22 Time series of the daily change in the normalized energy difference

Figure 23 shows the normalized energy difference between the control and test PV.

The data of interest is in blue (marked by o). Data in green (marked by ∇) was not used because the control PV was not cleaned. Data in red (marked by X) was not used (because of rain during December, January and April, and maintenance during June).

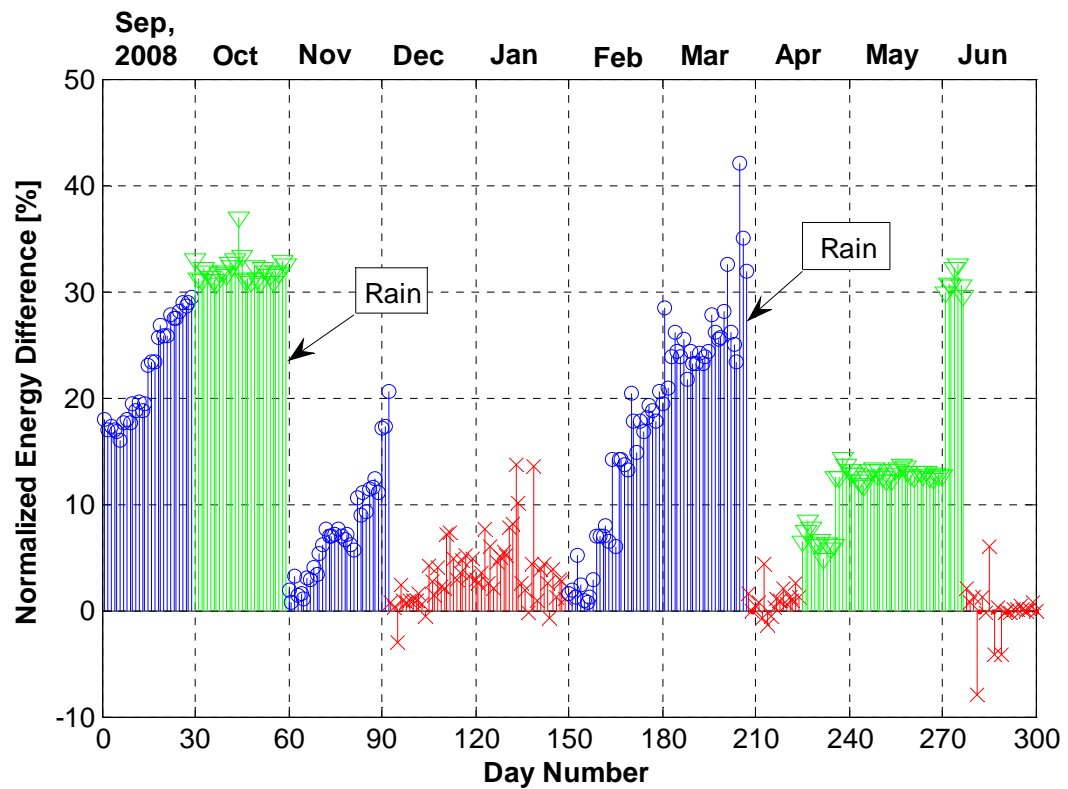


Figure 23 Normalized energy difference

3.3.3 THE EFFECT OF WIND SPEED

Figure 24 shows a scatter plot of the daily average wind speed against the daily change; no clear relationship can be inferred. Both deposition and resuspension fluxes of different magnitudes seem to happen at all wind speeds. In order to be able to understand the effect of wind speed on dust accumulation, wind speed has to be studied with all other variables kept constant. This can be achieved by filtering our data points into groups having constant values of other weather conditions. Using daily mean values of weather conditions, for reasons that we will explain in the following sections, resulted in a low number of data points which limited our ability to statistically verify the effect of wind speed on the daily change.

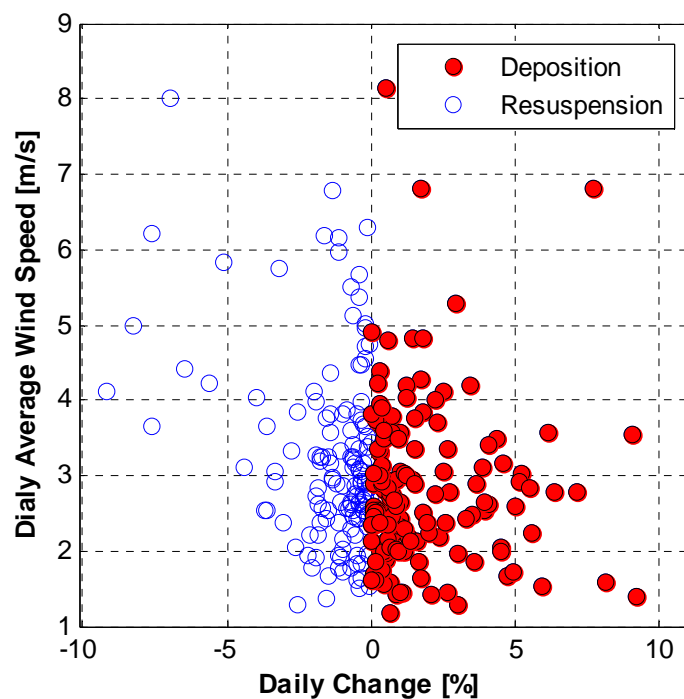


Figure 24 Scatter plot of daily change vs. daily average wind speed

3.3.4 THE EFFECT OF WIND DIRECTION

Figure 25 shows a scatter plot of the daily average wind direction against the daily change. As in the case of wind speed, there was no clear relationship between the wind direction and the daily change since the other weather parameters were not kept constant. By filtering the data set into groups where weather conditions other than the wind direction are kept constant, the effect of wind speed becomes clearer. In the following sections we will qualitatively explain our preliminary results and will explain how we can improve our experimental setup to quantitatively verify our model.

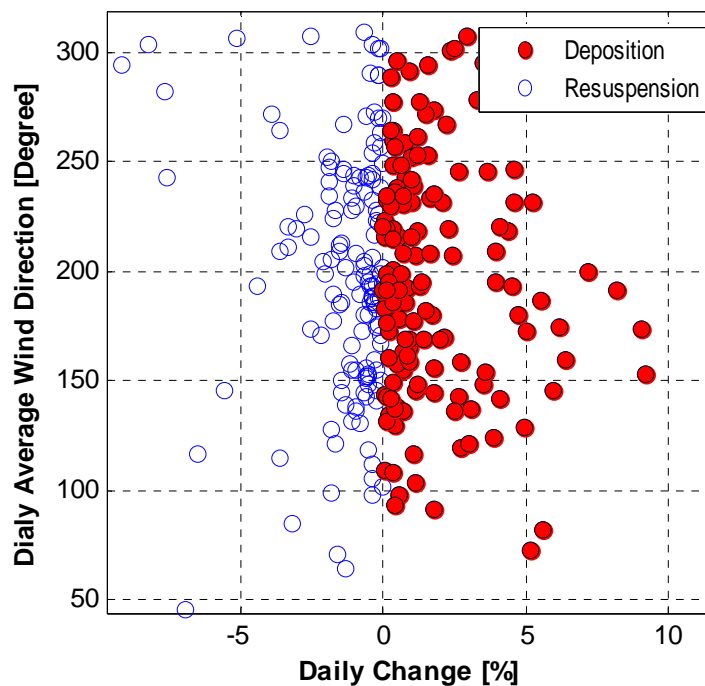


Figure 25 Scatter plot of daily change vs. daily average wind direction

3.4 PRELIMINARY RESULTS

It is clear from the test periods of interest in Figure 23 (blue marked by o) that:

- 1- A value of about 15 % per month of drop in energy occurs when the test PV is not cleaned.
- 2- The dust level did not reach a plateau even over a period of two months (e.g. February & March having a mean atmospheric dust concentration of 460 [$\mu\text{g}/\text{m}^3$]).

Although the mean energy drop per month was almost constant, we are interested to model the variation in energy on shorter time scales. When correlating atmospheric dust concentration, wind speed and wind direction with the type and magnitude of dust flux the following was observed:

- 1- For days having the same dust concentration, the mean wind speed during days having a net deposition of dust seems to be lower than that on days having a net resuspension of dust regardless of wind direction.
- 2- The value of the critical wind speed, below which we will have a net deposition and above which we will have a net resuspension, seems to be dependent on the dust concentration. This wind speed can be considered analogous to the minimum friction velocity needed to cause the minimum wind stress required to induce resuspension [36].
- 3- Also, for days having the same dust concentration, wind coming over the slope of the PV causes a higher magnitude of deposition than wind flowing parallel to the surface, while wind parallel to the surface of the PV causes higher magnitude of resuspension.

The previous preliminary qualitative analysis indicates that the measurement (or forecast) of atmospheric dust concentration, wind speed and wind direction can be used to predict dust accumulation as follows: for a certain dust concentration wind speeds can be used to identify the nature of the net flux (deposition or resuspension). It appears that the wind direction may affect the magnitude of flux. Nevertheless, we could not statistically verify our model and we will discuss this in the next section.

3.5 IMPROVING THE CURRENT EXPERIMENT

The previous results were not conclusive for different reasons. One of the major reasons was the lack of accurate measurements of atmospheric dust concentration. We inferred our atmospheric dust concentration from values of visibility. There was a limit on the range of the visibility data which translated into a limitation of the range of dust concentration.

Since we relied on the difference in the power output of the control and test PV to infer the amount of dust accumulation, we can only use this method during daytime where we have power output but not during the nights. We therefore had to take a mean daily difference in energy. Taking daily mean values of our measured parameters resulted in relatively low data points and we were not able to statistically verify our model.

Using daily mean values also limited our ability to study some other weather parameters such as humidity, which, we believe, also has a big effect on dust accumulation. The reason is that there is a large difference in the humidity values between days and nights. By using daily mean values for humidity (indicated in red

line in Figure 26), we will lose important information. Figure 26 shows the effect of using the daily mean humidity.

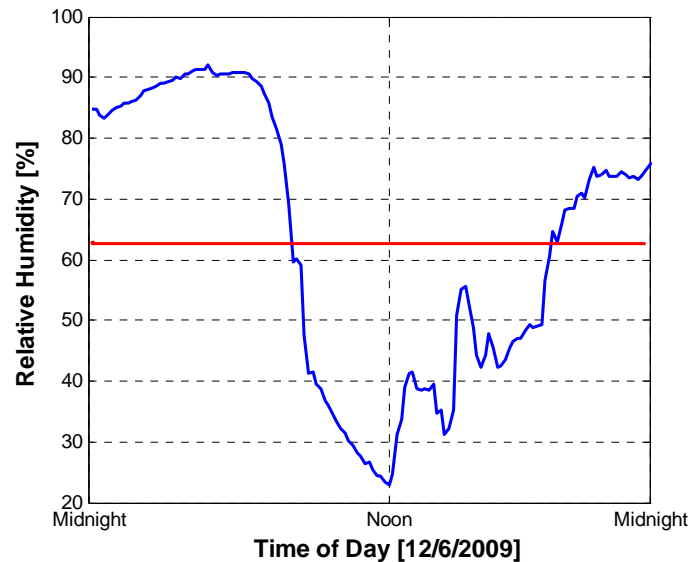


Figure 26 Effect of averaging humidity

The original data set also lacked an important parameter which is the formation of dew on the surface of the PV, which we also believe affects dust accumulation.

A new experimental setup is proposed to overcome the previous problems. The use of a real time aerosol sampler will provide high resolution and accurate measurements of atmospheric dust concentration.

Since during nights we don't have an indication of dust accumulation (the power output of the PVs is zero), we can cover the PVs at night to prevent any dust accumulation, eliminating the need of using daily mean values of weather conditions.

This will enable us to use high time resolution data and thus we may be able to statistically verify our model.

The formation of dew on the surface of the PV can be studied by using a surface humidity sensor, which indicates the formation of dew on a surface. Such a sensor is called a “wet leaf sensor”. Figure 27 is an example of a wet leaf sensor.



Figure 27 Wet leaf sensor

We are confident that our suggested improved experimental setup will enable us to better understand and develop a model that describes dust accumulation as a function of various weather conditions. The new experimental setup will provide us with the necessary high time resolution data that we need to statistically validate our model.

CHAPTER 4

Self-Cleaning Surface Testing

As discussed in chapter 1, in order to make the best use of the solar resource available, PV panels (and any other solar collector) needs constant cleaning. We also discussed several ways that can be used to clean the solar collectors. Using passive methods of cleaning such as using the so called self-cleaning surfaces translates into less maintenance, less time consumption and more ease. Any self-cleaning coating should be suitable for the specific region to be utilized in.

This chapter describes a test of the self-cleaning properties of a commercial hydrophobic coating for PVs. The investigation took place in the International PV Competition Test Field, Masdar City, Abu Dhabi.

4.1 METHODOLOGY

We divided our study into two parts: 1- surface characterization of the coating and 2- outdoor testing of the self-cleaning properties of the coating.

The surface characterization included testing of the optical and the morphological properties of the coating, and the water contact angle. In this part of the experiment the coating was applied on a small glass sample and the coating was then studied.

At the same time outdoor testing was performed by comparing the power output between two identical PV modules: a coated and uncoated one. The outdoor test took place starting from the 9th of December, 2010 till 31st of the same month.

4.2 TEST PROCEDURES

4.2.1 TOPOGRAPHY

Surface topography analysis was done using Atomic Force Microscopy (Asylum Research AFM). Figure 28 shows an AFM image that compares the surface morphology of the uncoated glass (left) and the coated glass (right). The coating creates a nano-structure on the surface of the glass that causes the water contact angle to increase according to Wenzel's equation [37] creating a hydrophobic surface. Analysis of the surface roughness showed that the coating increased the surface roughness (R_a) of our glass sample from 1.5 [nm] to 15.1 [nm] which created a hydrophobic surface.

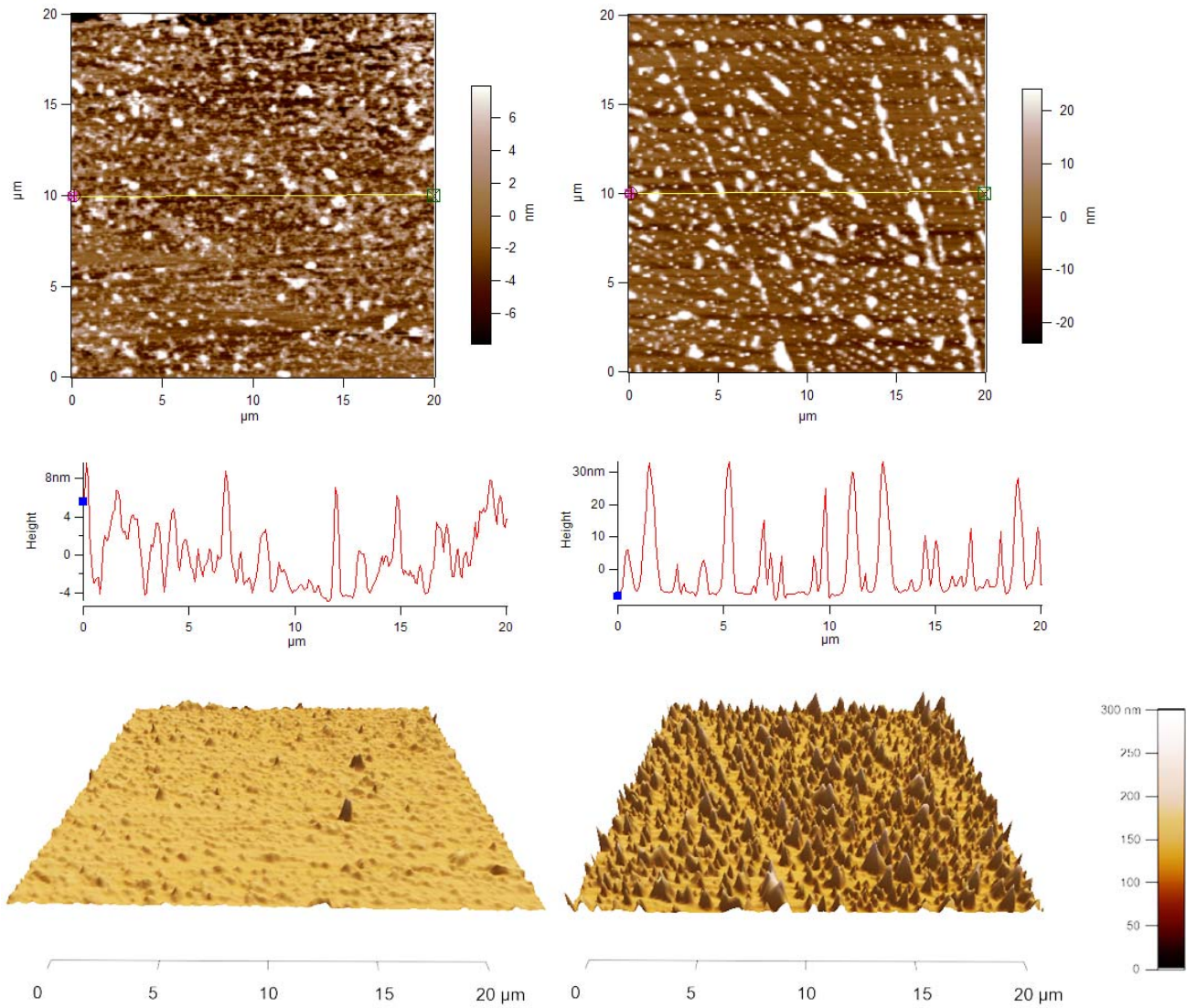


Figure 28 Top: AFM scan of the uncoated (left) and coated (right) glass cover. Middle: A cross section of the surface topography at the yellow line. Bottom: a 3-D scan of the uncoated (left) and coated (right) surfaces using the same scale.

4.2.2 CONTACT ANGLE MEASUREMENTS

As we have mentioned in chapter one, studies show that surfaces with high water contact angles may be utilized as a method to achieve coatings that minimize dust accumulation (the so called self-cleaning coatings). Therefore it was necessary to compare the water contact angle of our glass sample before and after applying the coating.

The contact angle was measured using a Goniometer (KRUS – EasyDrop system) by utilizing the static sessile drop method.

The contact angle measurements showed that the contact angle increased from 31° of the uncoated glass (Figure 29) to 110° after applying the coating (Figure 30).

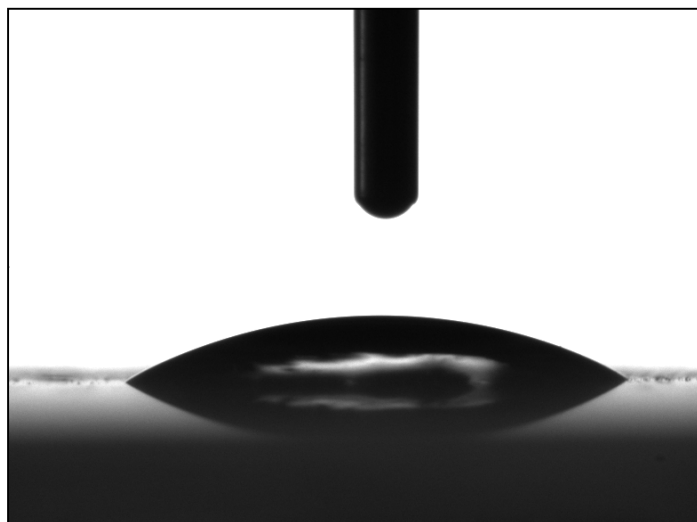


Figure 29 Contact angle of water on glass

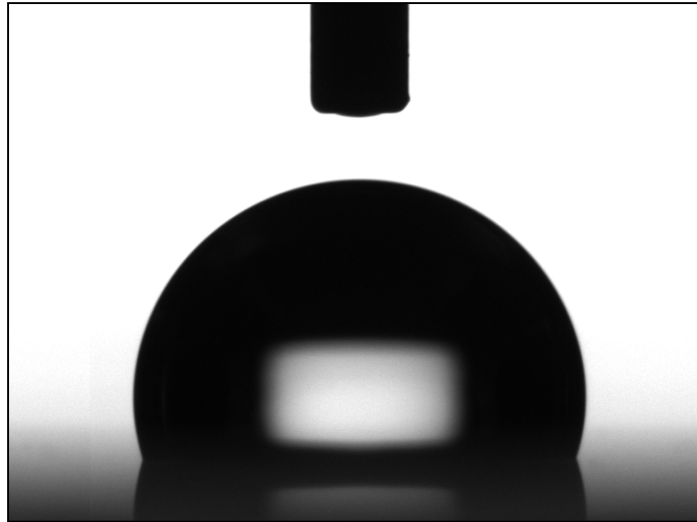


Figure 30 Contact angle of water on the nano-coating

4.2.3 OPTICAL PROPERTIES

It is very important to ensure that the PV module surface treatment does not affect the transmittance of the PV glass cover. We tested the optical properties of the coating using two different techniques. The first test³ employs three identical Licors⁴ (pyranometers) were used to compare the values of solar irradiation, solar irradiation through an uncoated glass and solar irradiation through a coated glass.

Figure 31 shows the Licor setup, with one extra Licor. Two Licors were covered with glass slides (coated and uncoated).

³ We chose this method in comparing between the transmittance of the coated and uncoated glass to take into account the incident angle modifier of the glass, and to simulate real spectrum conditions.

⁴ A pyranometer is an instrument for measuring solar radiation received from a whole hemisphere. It is suitable for measuring global sun plus sky radiation. <http://www.licor.com>

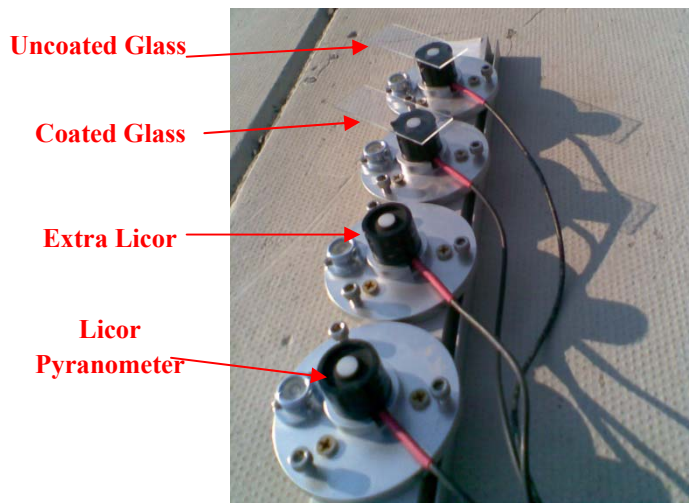


Figure 31 Experimental setup for testing for light transmittance

Output of the Licors was recorded over several days. There was no observed difference between the measured values of the irradiation of the Licor that was covered with the uncoated and coated glass. Figure 32 shows one sample day of the power output. It can be seen that the power output through the coated and uncoated glass is almost the same. This shows that the coating had no significant effect on the transmittance of light.

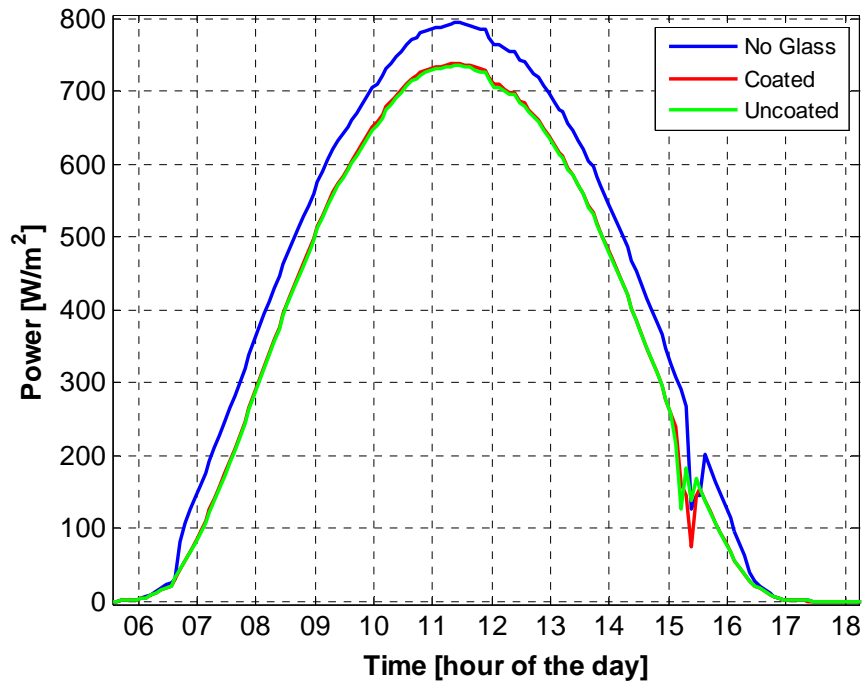


Figure 32 Power output of the uncovered and covered Licors

We also used a photospectrometer (Lambda 1050) to test the transmittance of the coated glass over a wide range of the spectrum (200 nm – 3300 nm). There was no noticeable difference between the results from the coated and uncoated glass.

4.2.4 OUTDOOR TESTING

The effectiveness of any coating boils down to its ability to reduce dust accumulation or reduce the amount of water necessary to clean the PV modules. For this reason, we compared the daily energy output of a coated and uncoated module at the international PV test field located at Masdar City, Abu Dhabi. The two modules are

identical⁵ and are connected to the grid through separate maximum power point trackers. Their maximum power output was recorded every 5 minutes. Figure 33 shows the daily energy output of the coated and uncoated PVs. As it can be seen there is no significant difference in the output of the two modules, which indicates that the coating is not decreasing dust accumulation.

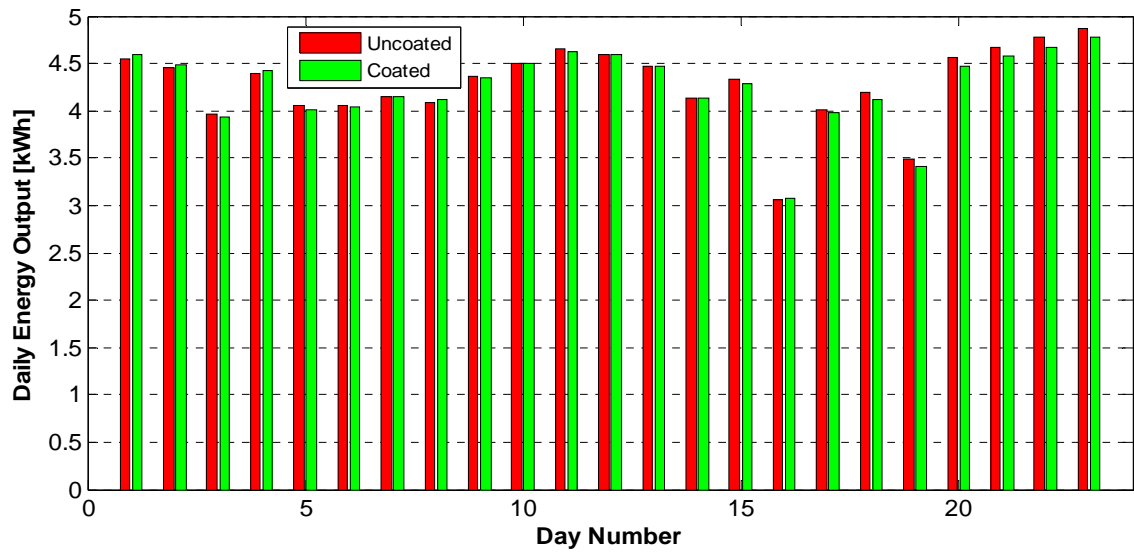


Figure 33 Daily Energy output of the coated and uncoated PV

⁵ On a clear day where both modules are clean, $b = P_{PV \text{ system } 1} / P_{PV \text{ system } 2} = 1.003$, and the coefficient of variation of the RMSE for $(P_{PV \text{ system } 1} - b * P_{PV \text{ system } 2}) / P_{PV \text{ system } 1} = 0.41 \%$. (Figures for a sample day: 12th, Dec 2008).

4.3 RESULTS AND CONCLUSIONS

Surface characterization shows that the coating forms a nano-structure that gives the hydrophobic property. Moreover, tests showed that the coating did not affect the transmittance of light. Outdoor testing shows that the daily energy output of the two systems is nearly identical⁶ over a period of 23 days. There was no significant difference between the cumulative energy collected by the uncoated and coated PV modules, and the mean cumulative energy difference per day was 24 [Wh]. This means that the coating did not reduce the dust accumulation.

There is a number of possible reasons for these findings. Studies have shown that the contact angle of some materials can change when subjected to UV rays. As an example Subedi [38] discusses how the UV treatment of polycarbonate enhances its wettability (decreases its contact angle). This may give us a possible indication that the coating's contact angle was reduced when it was used outdoors. It is also possible that the coating could not function properly under the high temperatures of Abu Dhabi.

It is suggested by Parkin [24] that in order to achieve self-cleaning properties, the static contact angle of the water on the coating should be very high forming a super hydrophobic surface. It is suggested that the rolling motion of the water droplet more efficiently cleans the surface and less likely to leave dust particles behind than the sliding motion that happens at a lower contact angles. The condition for such a super hydrophobic surface is often quoted as being larger than 160° , while the water contact angle of our coating is 110° . This might be another reason that could explain the results that we obtained.

⁶ Mean daily energy output = 4.25 kWh. $b = E_{\text{Daily,coated PV}} / E_{\text{Daily,uncoated PV}} = 1.006$, RMSE = 0.067 kWh.

In conclusion, extensive testing both indoors and outdoors are necessary to verify the self-cleaning ability of any coating. The composition and manufacturing process of the coating will directly affect factors such as its water contact angle, light transmittance, heat and UV resistance, all of which will affect its performance to reduce dust accumulation.

In any study to assess the performance of a coating, the coating should not be looked at alone. Dust accumulation is a result of the interaction of the dust particles with the surface. Therefore the type of dust should also be taken into account. Furthermore, other variables such as weather conditions (e.g. light transmittance, high temperature) should be kept in mind when testing any coating.

Understanding the process of dust accumulation and its relationship with the chemistry and morphology of the coating is important to develop a successful surface treatment. It should be noted that in our current study, we were not able to go further in analyzing the coating since the company that supplied the coating did not share the composition of the coating with us.

CHAPTER 5

Summary and Conclusions

5.1 SUMMARY

The objective of this research was to develop a model that describes dust accumulation in order to understand the factors that affect the utilization of PVs in an area with high dust concentrations. We started by developing a simple regression model that describes the power output of a PV, and then using a simple technique we were able to correct for the effect of incident angle without the need for any experimental work (described in chapter 2).

Then we moved on to tackle the problem of dust accumulation by trying to relate the rate of dust accumulation to different weather conditions. Our data set limited our

ability to statistically verify our model. Therefore, we described ways in which we can improve our experimental setup and the different parameters that need to be studied in order to be able to develop a model that describes dust accumulation (described in chapter 3).

We then explained the importance of assessing any cleaning method to be used in real outdoor conditions. We did that by describing a test we carried out to assess the self-cleaning properties of a commercial coating and explained the different parameters that need to be taken into account when assessing any coating with self-cleaning properties (described in chapter 4).

5.2 CONCLUSIONS AND RECOMMENDATIONS

5.2.1 *MODELING PV POWER OUTPUT*

A simple regression model and a methodology to correct the model for the effect of the incident angle were developed. The model should be further verified by using a year's data of power output, which is being collected at the moment. Different PV technologies should also be investigated and their power output should be compared against modeled values.

5.2.2 *DUST ACCUMULATION*

The preliminary qualitative analysis indicates that the measurement (or forecast) of atmospheric dust concentration, wind speed and wind direction can be used to predict dust accumulation as follows: for a certain dust concentration wind speeds can be used to identify the nature of the net flux (deposition or resuspension). It appears that the wind direction may affect the magnitude of flux.

In our work we used daily mean values for weather conditions and tried to relate them to daily variation in the normalized energy difference. This resulted in a low number of data points which made it difficult to identify the critical wind speed and wind direction values that are thought to control the sign and magnitude of the dust flux. For prediction purposes, average values over shorter time scales (e.g. 10 minute data) should be used. Future work includes modifying the experimental setup by adding a real time aerosol sampling instrument. This will enable analysis at a higher time resolution and could lead to a statistically valid model. Such a model has important potential of being used in the PV industry for forecasting PV performance at different locations subjected to various cleaning scenarios.

5.2.3 *FUNCTIONALIZED COATINGS*

In this part of the work we tested a functionalized commercial coating that was claimed to reduce the accumulation of dust on PVs. both indoor and outdoor testing was conducted.

Indoor testing included testing water contact angle, light transmittance and surface roughness of the coating. In the outdoor testing, we compared the energy yields of two identical PV modules: coated and uncoated PVs. When tested outdoors the coating did not give expected results.

Variables such as the composition and manufacturing process of the coating, the type of dust, weather conditions (e.g. humidity and temperature) and their interactions should be studied thoroughly to be able to develop a coating having self-cleaning properties.

It should be noted that further investigations of this problem were held back by the fact that the company that supplied the coating did not wish to share the composition of the coating with Masdar Institute.

Bibliography

- [1] A. Y. Al-Hasan, "A new correlation for direct beam solar radiation received by photovoltaic panel with sand dust accumulated on its surface," *Solar Energy*, vol. 63, no. 5, pp. 323-333, Nov. 1998.
- [2] A. A. Hegazy, "Effect of dust accumulation on solar transmittance through glass covers of plate-type collectors," *Renewable Energy*, vol. 22, no. 4, pp. 525-540, Apr. 2001.
- [3] A. M. El-Nashar, "Effect of dust deposition on the performance of a solar desalination plant operating in an arid desert area," *Solar Energy*, vol. 75, no. 5, pp. 421-431, Nov. 2003.
- [4] H. K. Elminir, A. E. Ghitas, R. H. Hamid, F. El-Hussainy, M. M. Beheary, and K. M. Abdel-Moneim, "Effect of dust on the transparent cover of solar collectors," *Energy Conversion and Management*, vol. 47, no. 18-19, pp. 3192-3203, Nov. 2006.
- [5] M. S. El-Shobokshy, A. Mujahid, and A. K. M. Zakzouk, "Effects of dust on the performance of concentrator photovoltaic cells," *Solid-State and Electron Devices, IEE Proceedings I*, vol. 132, no. 1, pp. 5-8, 1985.
- [6] M. Vivar et al., "Effect of soiling in CPV systems," *Solar Energy*, vol. 84, no. 7, pp. 1327-1335, Jul. 2010.
- [7] A. M. El-Nashar, "Seasonal effect of dust deposition on a field of evacuated tube collectors on the performance of a solar desalination plant," *Desalination*, vol. 239, no. 1-3, pp. 66-81, Apr. 2009.
- [8] P. Lengweiler, "Modelling Deposition and Resuspension of Particles on and from Surfaces," Swiss Federal Institute of Technology Zürich, 2000.
- [9] D. Goossens and Z. Y. Offer, "Comparisons of day-time and night-time dust accumulation in a desert region," *Journal of Arid Environments*, vol. 31, no. 3, pp. 253-281, Nov. 1995.
- [10] M. S. El-Shobokshy and F. M. Hussein, "Degradation of photovoltaic cell performance due to dust deposition on to its surface," *Renewable Energy*, vol. 3, no. 6-7, pp. 585-590, 1993.
- [11] D. Goossens and E. Van Kerschaever, "Aeolian dust deposition on photovoltaic solar cells: the effects of wind velocity and airborne dust concentration on cell performance," *Solar Energy*, vol. 66, no. 4, pp. 277-289, Jul. 1999.

- [12] B. Kroposki, K. Emery, D. Myers, and L. Mrig, "A comparison of photovoltaic module performance evaluation methodologies for energy ratings," in *Proceedings of 1994 IEEE 1st World Conference on Photovoltaic Energy Conversion - WCPEC (A Joint Conference of PVSC, PVSEC and PSEC)*, Waikoloa, HI, USA, pp. 858-862.
- [13] D. R. Myers, *Evaluation of the Performance of the PVUSA Rating Methodology Applied to Dual Junction PV Technology: Preprint (Revised)*. National Renewable Energy Laboratory (NREL), Golden, CO., 2009.
- [14] C. M. Whitaker et al., "Application and validation of a new PV performance characterization method," in *Photovoltaic Specialists Conference, 1997., Conference Record of the Twenty-Sixth IEEE, 1997*, pp. 1253–1256.
- [15] C. M. Whitaker, T. U. Townsend, H. J. Wenger, A. Iliceto, G. Chimento, and F. Paletta, "Effects of irradiance and other factors on PV temperature coefficients," in *Photovoltaic Specialists Conference, 1991., Conference Record of the Twenty Second IEEE, 1991*, pp. 608-613 vol.1.
- [16] E. L. Meyer and E. E. Van Dyk, "Development of energy model based on total daily irradiation and maximum ambient temperature," *Renewable energy*, vol. 21, no. 1, pp. 37–47, 2000.
- [17] B. Kroposki, W. Marion, D. L. King, W. E. Boyson, and J. A. Kratochvil, "Comparison of module performance characterization methods," in *Photovoltaic Specialists Conference, 2000. Conference Record of the Twenty-Eighth IEEE, 2000*, pp. 1407-1411.
- [18] K. Emery, B. Kroposki, B. Marion, D. Myers, and C. Osterwald, "Validation of a Photovoltaic Module Energy Ratings Procedure at NREL," 1999., 1999.
- [19] D. L. King, J. A. Kratochvil, and W. E. Boyson, *Photovoltaic array performance model*. United States. Dept. of Energy, 2004.
- [20] E. Skoplaki and J. A. Palyvos, "On the temperature dependence of photovoltaic module electrical performance: A review of efficiency/power correlations," *Solar energy*, vol. 83, no. 5, pp. 614–624, 2009.
- [21] M. Ma and R. M. Hill, "Superhydrophobic surfaces," *Current opinion in colloid & interface science*, vol. 11, no. 4, pp. 193–202, 2006.
- [22] C.-T. Hsieh, W.-Y. Chen, F.-L. Wu, and W.-M. Hung, "Superhydrophobicity of a three-tier roughened texture of microscale carbon fabrics decorated with silica spheres and carbon nanotubes," *Diamond and Related Materials*, vol. 19, no. 1, pp. 26-30, Jan. 2010.
- [23] Y.-B. Park, H. Im, M. Im, and Y.-K. Choi, "Self-cleaning effect of highly water-repellent microshell structures for solar cell applications," *Journal of Materials Chemistry*, vol. 21, no. 3, p. 633, 2011.
- [24] I. P. Parkin and R. G. Palgrave, "Self-cleaning coatings," *Journal of materials chemistry*, vol. 15, no. 17, pp. 1689–1695, 2005.

- [25] A. S. for T. and Materials, *Annual book of A.S.T.M. standards*. ASTM, 2007.
- [26] D. L. King, J. A. Kratochvil, and W. E. Boyson, “Measuring solar spectral and angle-of-incidence effects on photovoltaic modules and solar irradiance sensors,” in *Photovoltaic Specialists Conference, 1997., Conference Record of the Twenty-Sixth IEEE*, 1997, pp. 1113–1116.
- [27] L. Castañer and S. Silvestre, *Modelling photovoltaic systems using PSpice*. John Wiley and Sons, 2002.
- [28] J. A. Duffie and W. A. Beckman, *Solar engineering of thermal processes*. Wiley, 2006.
- [29] B. Marion, “Comparison of predictive models for photovoltaic module performance,” in *Photovoltaic Specialists Conference, 2008. PVSC’08. 33rd IEEE*, pp. 1–6.
- [30] G. J. Myatt, *Making sense of data: a practical guide to exploratory data analysis and data mining*. John Wiley and Sons, 2007.
- [31] LI-COR, “LI-COR Terrestrial Radiation Sensors - Instruction Manual.” .
- [32] Y. Shao, *Physics and Modelling of Wind Erosion*. Springer, 2008.
- [33] W. C. Hinds, *Aerosol technology: properties, behavior, and measurement of airborne particles*. Wiley, 1999.
- [34] Y. Shao et al., “Northeast Asian dust storms: Real-time numerical prediction and validation,” *Journal of Geophysical Research*, vol. 108, p. 18 PP., Nov. 2003.
- [35] Y. Shao and C. H. Dong, “A review on East Asian dust storm climate, modelling and monitoring,” *Global and Planetary Change*, vol. 52, no. 1-4, pp. 1-22, Jul. 2006.
- [36] O. J. Nielsen, *A literature review on radioactivity transfer to plants and soil*. Riso National Laboratory, 1981.
- [37] R. N. Wenzel, “Resistance of solid surfaces to wetting by water,” *Industrial & Engineering Chemistry*, vol. 28, no. 8, pp. 988–994, 1936.
- [38] D. P. Subedi, R. B. Tyata, and D. Rimal, “Effect of UV-Treatment on the Wettability of Polycarbonate.”